

Plateau Moduli of Several Single-Chain Slip-Link and Slip-Spring Models

Takashi Uneyama^{*} and Yuichi Masubuchi

Center for Computational Science, Graduate School of Engineering,
Nagoya University,
Furo-cho, Chikusa, Nagoya 464-8603, Japan
e-mail: uneyama@mp.pse.nagoya-u.ac.jp

Abstract

We calculate the plateau moduli of several single-chain slip-link and slip-spring models for entangled polymers. In these models, the entanglement effects are phenomenologically modeled by introducing topological constraints such as slip-links and slip-springs. The average number of segments between two neighboring slip-links or slip-springs, N_0 , is an input parameter in these models. To analyze experimental data, the characteristic number of segments in entangled polymers N_e estimated from the plateau modulus is used instead. Both N_0 and N_e characterize the topological constraints in entangled polymers, and naively N_0 is considered to be the same as N_e . However, earlier studies showed that N_0 and N_e (or the plateau modulus) should be considered as independent parameters. In this work, we show that due to the fluctuations at the short time scale, N_e deviates from N_0 . This means that the relation between N_0 and the plateau modulus is not simple as naively expected. The plateau modulus (or N_e) depends on the subchain-scale details of the employed model, as well as the average number of segments N_0 . This is due to the fact that the subchain-scale fluctuation mechanisms depend on the model rather strongly. We theoretically calculate the plateau moduli for several single-chain slip-link and slip-spring models. Our results explicitly show that the relation between N_0 and N_e is model-dependent. We compare theoretical results with various simulation data in the literature, and show that our theoretical expressions reasonably explain the simulation results.

1 Introduction

Polymer melts and solutions with sufficiently large molecular weights exhibit characteristic relaxation behaviors due to the “entanglements.” The entanglements originate from the non-crossability between polymer chains.¹ Polymer chains cannot cross each other, and thus the motion of a polymer chain is strongly constrained compared with freely crossable phantom chains. As a result, we observe various characteristic dynamical behaviors. For example, the longest relaxation time becomes very long and the relaxation modulus $G(t)$ of a well entangled polymer becomes approximately constant as $G(t) \approx G_N^{(0)}$ (with $G_N^{(0)}$ being a constant) in a relatively long time range before the system fully relaxes. The plateau modulus $G_N^{(0)}$ is an important parameter which characterizes the entanglement effect². The emergence of the plateau modulus can be phenomenologically interpreted as the existence of a transient rubber-like network in an entangled polymer system. Experimentally, we can directly measure the plateau modulus $G_N^{(0)}$ if the molecular weight is sufficiently large and polymers are well-entangled. Even if the molecular weight is not sufficiently large, several methods have been developed to estimate the plateau modulus from the linear viscoelasticity data³. Therefore, from the experimental view point, we can say that the plateau modulus of a specific polymer can be determined straightforwardly. If we assume that an entangled polymer simply behaves as an ideal rubber network, we can estimate the average molecular weight between

(virtual) cross-links. This molecular weight can be interpreted as the molecular weight between entanglements (the molecular weight between two sequential transient linking points) M_e .

However, the situation is not that clear in mesoscopic coarse-grained models. In most of mesoscopic coarse-grained simulation models for entangled polymers, the entanglements are phenomenologically implemented as some transient objects (such as tubes and slip-links).¹ In such models, the molecular weight between entanglements is interpreted as an input parameter. We express the molecular weight between two entanglement points in coarse-grained models as M_0 . Naively one may expect that M_e from the plateau modulus is just the same as the molecular weight between two entanglement points M_0 ($M_e = M_0$). However, this is not true in general. We should emphasize that M_0 cannot be experimentally observed (unlike M_e). The relation between M_0 and $G_N^{(0)}$ depends on the details of the employed model. Although the relation between M_e and $G_N^{(0)}$ has been studied in detail for some specific models⁴, this relation is not clear for most of coarse-grained models. As a result, to fit simulation data of mesoscopic coarse-grained models to specific experimental data, sometimes we are required to use both M_0 and $G_N^{(0)}$ as independent fitting parameters^{5,6}. This procedure works well for practical purposes, but it seems not to be fully consistent with a naive and intuitive interpretation of M_0 .

We should carefully consider the relation between M_0 and $G_N^{(0)}$ in mesoscopic coarse-grained models. For example, in the tube model, the value of $G_N^{(0)}$ is known to be reduced if we take into account the longitudinal motion of a chain along the tube¹. If we interpret an entangled polymer system as a network, the functionality of this network also affects the plateau modulus, in the same way as the phantom network^{7,8}. In this work, we theoretically investigate the plateau modulus for various slip-link and slip-spring type models in detail. Although the plateau modulus apparently seems to be well-defined, from the theoretical view point, how to determine the plateau modulus is not fully clear. In this work, we define the plateau modulus $G_N^{(0)}$ from the relaxation modulus $G(t)$ as:

$$G_N^{(0)} \equiv G(t \approx \tau_e). \quad (1)$$

Here, we should use $G(t)$ for a well entangled system of which molecular weight is sufficiently large. This definition is almost the same as the “entanglement modulus G_e ” proposed by Likhtman and McLeish⁹. Because most of mesoscopic coarse-grained models employ segments as fundamental units (rather than monomers), it would be convenient to use the number of segments between entanglements N_e , instead of the molecular weight between entanglements M_e . (Here, we assume the Kuhn segment as the segment for coarse-grained models.) In the same way, we employ N_0 to express the segment number between two sequential slip-linked or slip-springed points. We define the average number of segments between entanglements from eq (1) via the classical rubber elasticity formula (so-called the Ferry type definition)^{1,9,10}:

$$N_e \equiv \frac{\rho_0 k_B T}{G_N^{(0)}}, \quad (2)$$

where ρ_0 is the number density of segments, k_B is the Boltzmann constant, and T is the temperature.

The segment number between entanglements N_e defined by eq (2) can be interpreted as the characteristic segment number of a model, and naively we expect N_e to be the input parameter. However, as mentioned, generally $N_0 \neq N_e$. Thus if we simply set $N_0 = N_e$, the plateau modulus of a model deviates from eq (2). Although this problem itself has been recognized by researchers⁶, as far as the authors know, the relation between N_0 and $G_N^{(0)}$, or, equivalently, the relation between N_0 and N_e is still not well understood (except a few limited systems⁴).

There are various similar but different mesoscale coarse-grained models for entangled polymers. To quantitatively compare or connect different models, the relation between N_0 and $G_N^{(0)}$ (or N_e) is important. (For example, N_0 of one model may be quantitatively different from N_0 of another model, even if two models give the same plateau modulus.) In this work, we theoretically calculate the relation between N_0 and $G_N^{(0)}$ for various single-chain slip-link and slip-spring type models. We calculate the plateau modulus under the assumption that the subchain-scale structures are fully

relaxed but the slip-links and slip-springs are not reconstructed. We show that the plateau modulus $G_N^{(0)}$ depends on several parameters such as the interaction model between slip-links and the spring constant of slip-springs. We also perform Monte Carlo simulations to examine the accuracy of our theoretical predictions. Our results suggest that the various relaxation mechanisms affect the value of $G_N^{(0)}$. This makes the relation between N_0 and $G_N^{(0)}$ (or N_e) strongly model-dependent. We examine some literature data and discuss how we should interpret the simulation data obtained by molecular dynamics models and mesoscopic coarse-grained models.

2 Model

2.1 Equilibrium Probability Distribution

In this work, we consider slip-link and slip-spring type models. In these models, the entanglement effect is mimicked by introducing transient objects which work like cross-links. These transient objects are called the slip-links or slip-springs. Various slip-link and slip-spring type models have been proposed for entangled polymer systems^{11–19}. Although these models can reproduce characteristic dynamics of entangled polymers, they are not equivalent. They are phenomenologically designed based on similar but different assumptions, and thus their statistical properties are different. As far as a model can reasonably reproduce some dynamic quantities such as the relaxation modulus, we can employ any model. Here we do not limit ourselves to a specific model and study some different models.

To make the analyses tractable, in this work we limit ourselves to the single-chain type models. In a single-chain slip-link model, we consider the dynamics of a single tagged chain and assume that the slip-links are attached to the tagged chain. A segment to which a slip-link is attached is spatially fixed and cannot move freely. (This corresponds to the affine network model in the rubber elasticity theory.) The polymer chain is allowed to slip (slide) through slip-links, and if a slip-link reaches to the chain end, it is destroyed. To compensate the destroyed slip-links, slip-links can be newly constructed and put on the chain. In the rubber elasticity theory, the fluctuation of the cross-links affects the modulus. Therefore, models with fluctuations of slip-linked points would be preferred. To incorporate the fluctuations of slip-linked points, we employ the slip-spring models in this work. In the case of a single-chain slip-spring model, slip-links are replaced by slip-springs. One end of a slip-spring is fixed in space (just like the case of a slip-link), and another end is attached to a segment. Two ends of a slip-spring is connected by a harmonic spring. (The positions of slip-springed points on the chain can fluctuate in space, and we expect that this may mimic the non-affine network models such as the phantom network model, in some aspects.) The slip-springs can be dynamically destroyed and constructed in the same way as slip-links. These slip-link and slip-spring models can reproduce various characteristic dynamical behaviors of entangled polymers. The rheological properties of a model depend both on static properties (such as the interaction potential model) and dynamic properties (such as the dynamic equations and transition models). As we show in the following subsection, however, the details of dynamics is not so important for the calculation of the plateau modulus. We need only the equilibrium probability distribution function to calculate the plateau modulus.

Without slip-links and slip-springs, a tagged chain is simply modeled as an ideal Gaussian chain. It would be fair to mention that the Gaussian chain statistics is not always reasonable. For example, if the chain is stiff, we should replace the Gaussian chain statistics by other statistics such as a freely jointed chain model and models with the bending rigidity. In this work we limit ourselves to the Gaussian chain statistics which is the simplest and suitable to theoretical analyses. For simplicity, in this work we assume that the total number of segments in a chain, N , is given as a multiple of N_0 , as $N = N_0 Z_0$ with Z_0 being a positive integer. (This assumption is not essential. The results are not changed even if N is not a multiple of N_0 . However, the expressions become a bit complicated in such a case.) Z_0 can be interpreted as the average number of slip-linked or slip-springed subchains in the tagged chain. Because we are interested in the plateau modulus, we assume that Z_0 is sufficiently large, $Z_0 \gg 1$. (This assumption makes the statistical properties somewhat simple.)

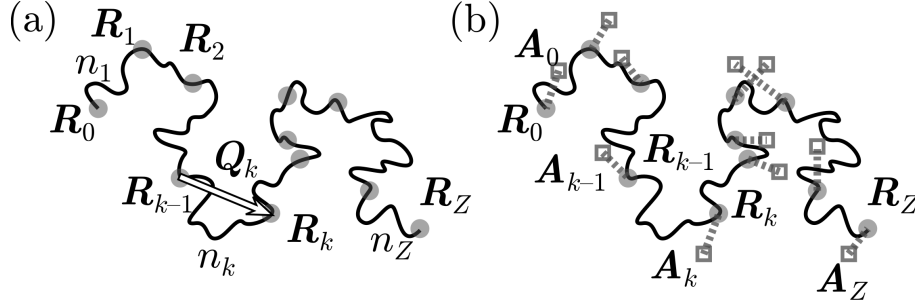


Figure 1: Schematic images of the single-chain slip-link and slip-spring models. (a) The slip-link model. Slip-links (gray circles) are attached to a Gaussian chain (the solid black curve). The polymer chain consists of Z subchains. \mathbf{R}_k and \mathbf{Q}_k represent the k -th slip-linked point and the k -th bond vector, respectively. n_k represents the number of segments in the k -th subchain. (b) The slip-spring model. Slip-springs (gray dotted lines) are attached to a Gaussian chain (the solid black curve). One end of a slip-spring is attached to the chain (a gray circle) whereas another end is anchored in space (a gray square). \mathbf{A}_k represents the anchoring point of the k -th slip-spring.

We start from the single-chain slip-link models. The state of the system (the tagged chain) is expressed by the positions of chain ends and slip-linked points, the number of segments in slip-linked subchains, and the total number of subchains. We express the number of subchains as Z ($Z = 1, 2, 3, \dots$) and the k -th constrained point on the chain as \mathbf{R}_k ($k = 0, 1, 2, \dots, Z$). $k = 0$ and Z correspond to the chain ends and others correspond to slip-linked points. The number of segments between the $(k-1)$ -th and the k -th points is expressed as n_k ($k = 1, 2, \dots, Z$). An image of a tagged chain with slip-links is depicted in Figure 1(a). For convenience, in what follows, we use dimensionless units. We set $\sqrt{N_0 b^2/3}$, N_0 , and $k_B T$ as the units of length, segment number, and energy. (This is equivalent to simply set $N_0 = 1$, $b^2/3 = 1$, and $k_B T = 1$.)

Even if we limit ourselves to the single-chain slip-link models, there are various similar but different models. For example, we can select the interaction potential model for slip-links, which directly affects the statistical properties²⁰. We start from the non-interacting slip-links. In this work, we call this model as an ideal slip-link model. The free energy of the ideal slip-link model is given as²¹

$$\mathcal{F}_{\text{IL}}(\{\mathbf{R}_k\}, \{n_k\}, Z) = \sum_{k=1}^Z \frac{\mathbf{Q}_k^2}{2n_k} + \sum_{k=1}^Z \frac{3}{2} \ln n_k. \quad (3)$$

Here, the subscript “IL” represents the ideal (“I”) slip-link (“L”) model. For convenience, we have introduced the bond vector $\mathbf{Q}_k \equiv \mathbf{R}_k - \mathbf{R}_{k-1}$ (see Figure 1(a)). The equilibrium probability distribution for the ideal slip-link model can be obtained by using the grand canonical type formulation for slip-links²¹. In the grand canonical type formulation, slip-links are treated as a sort of ideal gas particles in one dimension. The equilibrium probability distribution can be expressed as

$$P_{\text{eq,IL}}(\{\mathbf{R}_k\}, \{n_k\}, Z) = \frac{\xi^{Z-1} e^{-\xi}}{\mathcal{V}} \delta\left(Z_0 - \sum_{k=1}^Z n_k\right) \prod_{k=1}^Z \frac{1}{(2\pi n_k)^{3/2}} \exp\left[-\frac{\mathbf{Q}_k^2}{2n_k}\right], \quad (4)$$

where ξ is the effective fugacity (activity) for slip-links, and \mathcal{V} is the volume of the system. ξ is determined so that the equilibrium average number of subchains becomes Z_0 .

We also consider the single-chain slip-link models with the effective interaction between slip-links²⁰. Although there are many possible interaction potential models between slip-links, in this work we limit ourselves to two special cases. One is the effective repulsion potential which cancels the logarithmic term in eq (3). We call this model as the single-chain repulsive slip-link (“RL”) model. The repulsive slip-link model can be related to the primitive chain network (PCN) model¹², which is one of the multi-chain slip-link models. Some properties of the repulsive slip-link model can be directly utilized to study the PCN model. Another is a very strong repulsive potential,

with which slip-links form a sort of the Wigner crystal structure on the chain. We call this model as the single-chain equidistant slip-link (“EL”) model, because the number of segments between neighboring slip-links becomes constant and thus slip-links are placed equidistantly on the chain.

The free energy of the repulsive slip-link model is given as

$$\mathcal{F}_{\text{RL}}(\{\mathbf{R}_k\}, \{n_k\}, Z) = \mathcal{F}_{\text{IL}}(\{\mathbf{R}_k\}, \{n_k\}, Z) - \sum_{k=1}^Z \frac{3}{2} \ln n_k = \sum_{k=1}^Z \frac{\mathbf{Q}_k^2}{2n_k}. \quad (5)$$

Following the grand canonical type formulation, we have the formal expression for the equilibrium probability distribution of the repulsive slip-link model.

$$P_{\text{eq,RL}}(\{\mathbf{R}_k\}, \{n_k\}, Z) = \frac{\xi^{Z-1}}{\mathcal{V} E_{5/2,5/2}(\xi)} \delta\left(Z_0 - \sum_{k=1}^Z n_k\right) \frac{1}{(2\pi)^{3Z/2}} \exp\left[-\sum_{k=1}^Z \frac{\mathbf{Q}_k^2}{2n_k}\right] \quad (6)$$

where $E_{5/2,5/2}(x)$ is the generalized Mittag-Leffler function²² (the explicit form of $E_{5/2,5/2}(x)$ is not required for the calculations below). As before, the effective fugacity is determined so that the average number of subchains becomes Z_0 . Although eq (6) is not simple, if we focus on the statistics of just a single subchain in the system, the probability distribution can be largely simplified. (See Appendix A.) On the other hand, in the equidistant slip-link model, the equilibrium probability distribution function becomes quite simple:

$$P_{\text{eq,EL}}(\{\mathbf{Q}_k\}, \{n_k\}, Z) = \frac{\delta_{Z,Z_0}}{\mathcal{V}} \left[\prod_{k=1}^{Z_0} \delta(n_k - 1) \right] \frac{1}{(2\pi)^{3Z_0/2}} \exp\left[-\sum_{k=1}^{Z_0} \frac{\mathbf{Q}_k^2}{2}\right]. \quad (7)$$

Eq (7) means that the equidistantly slip-linked chain behaves as a simple bead-spring chain. (δ_{Z,Z_0} in eq (7) is the Kronecker delta which arises from the fact that Z is constant and cannot fluctuate in the equidistant slip-link model.)

In the single-chain slip-spring models, slip-linked points are allowed to fluctuate in space around their average positions (the anchoring points). One end of a slip-spring is attached to a slip-linked point on the chain, and another end is anchored in space. We express the anchoring point of the k -th slip-spring as \mathbf{A}_k ($k = 0, 1, \dots, Z$). An image of a tagged chain with slip-springs is depicted in Figure 1(b). A slip-spring is modeled as an entropic spring which can be interpreted as a short polymer chain. We express the number of segments for this short polymer chain as N_s . For simplicity, we also attach slip-springs to chain ends. (This does not affect the plateau modulus for a sufficiently long chain with $Z_0 \gg 1$.)

We consider three different interaction models between slip-springs, as the case of the slip-link models explained above. The free energy of the ideal slip-spring model is expressed as the sum of the free energy of the ideal slip-link model and the free energy of slip-springs:

$$\mathcal{F}_{\text{IS}}(\{\mathbf{R}_k\}, \{n_k\}, Z) = \mathcal{F}_{\text{IL}}(\{\mathbf{R}_k\}, \{n_k\}, Z) + \sum_{k=0}^Z \frac{(\mathbf{R}_k - \mathbf{A}_k)^2}{2\phi}. \quad (8)$$

The subscript “IS” represents the ideal slip-spring (“S”) model. Here, ϕ is the parameter which represents the effective size of slip-springs. (In dimensional units, ϕ is expressed as $\phi = N_s/N_0$.) We call ϕ as the “slip-spring size parameter” in the followings. The free energies for the repulsive and equidistant slip-spring (“RS” and “ES”) models can be constructed in the same way.

The equilibrium probability distributions for the single-chain slip-spring models can be constructed by utilizing the equilibrium probability distributions for the single-chain slip-link models. The equilibrium probability distribution for the anchoring points is given as a Gaussian distribution:

$$P_{\text{eq,S}}(\{\mathbf{A}_k\}|\{\mathbf{R}_k\}, \{n_k\}, Z) = \frac{1}{(2\pi\phi)^{3(Z+1)/2}} \exp\left[-\sum_{k=0}^Z \frac{(\mathbf{R}_k - \mathbf{A}_k)^2}{2\phi}\right]. \quad (9)$$

Here, $P_{\text{eq}}(X|Y)$ represents the conditional probability distribution of X under a given Y . The subscript “S” represents all the three slip-springs models (“IS”, “RS”, and “ES”). The equilibrium probability distribution of the slip-spring model is thus expressed as

$$P_{\text{eq,S}}(\{\mathbf{R}_k\}, \{\mathbf{A}_k\}, \{n_k\}, Z) = \frac{1}{(2\pi\phi)^{3(Z+1)/2}} \exp \left[- \sum_{k=0}^Z \frac{(\mathbf{R}_k - \mathbf{A}_k)^2}{2\phi} \right] P_{\text{eq,L}}(\{\mathbf{R}_k\}, \{n_k\}, Z). \quad (10)$$

The subscript “L” represents the slip-link models. (Eq (10) is common for all the three slip-spring models examined in this work.)

2.2 Linear Response Theory and Plateau Modulus

We can calculate the shear relaxation modulus by evaluating the relaxation process after the step deformation. Then the plateau modulus is determined by eq (1). Although this approach is intuitive, it requires us to evaluate the relaxation process directly. However, the relaxation process is generally model-dependent, and the analytic evaluation of the relaxation process is not easy. On the other hand, according to the linear response theory, the shear relaxation modulus of a given model can be evaluated systematically by evaluating the correlation function²³. The standard framework of the linear response theory is universal and we expect that we can proceed the calculation without knowing the details of the relaxation process. In this subsection, therefore, we derive the expression of the plateau moduli for the single-chain slip-link and slip-spring models from the view point of the linear response theory.

The linear response theory claims that the response function of a physical quantity can be expressed by using the correlation function of that physical quantity and another physical quantity which is conjugate to the applied external field. (In the case of the relaxation modulus, both of them are the shear stress.) For the single-chain slip-link models, the linear response theory gives

$$G(t) = \nu_0 \langle \hat{\sigma}_{xy}(t) \hat{\sigma}_{xy}(0) \rangle_{\text{eq}}. \quad (11)$$

where $\nu_0 \equiv \rho_0/Z_0$ is the average subchain number density and $\hat{\sigma}_{xy}(t)$ is the xy -component of the single-chain stress tensor at time t . $\langle \dots \rangle_{\text{eq}}$ means the statistical average in equilibrium. (The factor ν_0 represents the fact there are many polymer chains in a bulk system. The single-chain model gives the modulus just for a single chain. However, a bulk system consists of many statistically independent chains. We should introduce the factor ν_0 to reproduce the relaxation modulus correctly.) From the stress-optical rule, the single-chain stress tensor is simply given as follows:

$$\hat{\sigma}(t) = \sum_{k=1}^{Z(t)} \frac{\mathbf{Q}_k(t) \mathbf{Q}_k(t)}{n_k(t)}. \quad (12)$$

Here, the stress-optical coefficient is taken to be unity. Now we consider to calculate the plateau moduli of the slip-link models by eq (11). Clearly it is not easy to calculate $G(t)$ exactly. (It requires the detailed information of the dynamics.) Nevertheless, we are able to obtain accurate approximate expressions under several conditions. From eq (1), it is sufficient for us to calculate the value of $G(t)$ only around $t = \tau_e$. Besides, at this time scale, $G(t)$ is expected to be almost constant. At the time scale of $t \approx \tau_e$, we can reasonably assume that the slip-links are not constructed nor destroyed. Thus here we assume that the positions of slip-links are not changed. However, the transport of segments between neighboring subchains occurs even at the relatively short time scale. Thus we expect that the segment numbers in subchains are locally equilibrated at this time scale. We consider that only the segment numbers are equilibrated and other variables are unchanged at $t \approx \tau_e$. Then we can set $\mathbf{R}_k(t) = \mathbf{R}_k(0) = \mathbf{R}_k$ and $Z(t) = Z(0) = Z$ in eq (11), and assume that $\{n_k(0)\}$ and $\{n_k(\tau_e)\}$ are sampled independently from the local equilibrium distribution. Under these assumptions, the plateau modulus can be approximately expressed as

$$G_{N,L}^{(0)} \approx \nu_0 \sum_{Z=0}^{\infty} \int d\{\mathbf{R}_k\} \left[\int d\{n_k\} \sum_{k=1}^Z \frac{Q_{k,x} Q_{k,y}}{n_k} P_{\text{eq,L}}(\{n_k\} | \{\mathbf{R}_k\}, Z) \right]^2 P_{\text{eq,L}}(\{\mathbf{R}_k\}, Z). \quad (13)$$

For the single-chain slip-spring models, we should take into account the contribution of slip-springs (the virtual stress). The linear response formula becomes as follows^{24,25}:

$$G(t) = \nu_0 \langle \hat{\sigma}_{xy}(t) \hat{\sigma}_{xy}(0) \rangle_{\text{eq}} + \nu_0 \langle \hat{\sigma}_{xy}(t) \hat{\sigma}_{xy}^{(v)}(0) \rangle_{\text{eq}}. \quad (14)$$

Here $\hat{\sigma}_{xy}^{(v)}$ is the virtual stress tensor by slip-springs:

$$\hat{\sigma}^{(v)}(t) = \sum_{k=0}^{Z(t)} \frac{(\mathbf{R}_k(t) - \mathbf{A}_k(t))(\mathbf{R}_k(t) - \mathbf{A}_k(t))}{\phi}. \quad (15)$$

It would be fair to mention that the definition of the stress in the slip-spring models is not fully clear. From the linear response theory²⁵, $\hat{\sigma}_{xy} + \hat{\sigma}_{xy}^{(v)}$ is conjugate to the applied strain, and should be employed as the stress. However, $\hat{\sigma}_{xy} + \hat{\sigma}_{xy}^{(v)}$ is generally not consistent with the stress-optical rule. Thus, from the stress-optical rule, we should employ $\hat{\sigma}_{xy}$ as the stress tensor (as the case of the slip-link models). Here we assume that the stress-optical rule holds and employ $\hat{\sigma}_{xy}$ as the stress of the slip-spring models. This gives eq (14). At $t \approx \tau_e$, we expect that the positions $\{\mathbf{R}_k\}$ and segment numbers $\{n_k\}$ are locally equilibrated while other variables are unchanged. Then we have the following approximate expression for the plateau modulus:

$$\begin{aligned} G_{N,S}^{(0)} \approx & \nu_0 \sum_{Z=0}^{\infty} \int d\{\mathbf{A}_k\} \left[\int d\{\mathbf{R}_k\} d\{n_k\} \sum_{k=1}^Z \frac{Q_{k,x} Q_{k,y}}{n_k} P_{\text{eq},S}(\{\mathbf{R}_k\}, \{n_k\} | \{\mathbf{A}_k\}, Z) \right] \\ & \times \left[\int d\{\mathbf{R}_k\} d\{n_k\} \left[\sum_{k=1}^Z \frac{Q_{k,x} Q_{k,y}}{n_k} + \sum_{k=0}^Z \frac{(R_{k,x} - A_{k,x})(R_{k,y} - A_{k,y})}{\phi} \right] \right. \\ & \left. \times P_{\text{eq},S}(\{\mathbf{R}_k\}, \{n_k\} | \{\mathbf{A}_k\}, Z) \right] P_{\text{eq},S}(\{\mathbf{A}_k\}, Z). \end{aligned} \quad (16)$$

From the expressions shown above, we can calculate the plateau moduli of slip-link and slip-spring models only from the local equilibrium probability distributions.

3 Theory

3.1 Single-Subchain Approximation

To proceed the calculation and obtain the explicit expressions for the plateau moduli of the slip-link and slip-spring models, we employ the single-subchain approximation. We consider only a single tagged subchain in a chain. Such an approximation enables us to analytically calculate various statistical quantities including the plateau modulus.

For the single-chain slip-link models, the state of a single subchain can be fully expressed by the number of segments in the subchain and the bond vector of the subchain. We consider the k -th subchain as a tagged subchain and express $n = n_k$ and $\mathbf{Q} = \mathbf{Q}_k$ (as schematically shown in Figure 2(a)). The probability distribution function for a single subchain, $P_{\text{eq}}(\mathbf{Q}, n)$, is already obtained for several slip-link models.²⁰ The segment number distribution function $P_{\text{eq}}(n)$ and the bond vector distribution function $P_{\text{eq}}(\mathbf{Q})$ are calculated straightforwardly from $P_{\text{eq}}(\mathbf{Q}, n)$. We show the simple derivation which gives the same result as the previous work²⁰ in Appendix A. In the slip-link models, the segment number distribution function is given as follows:

$$P_{\text{eq},L}(n) = \begin{cases} e^{-n} & (\text{ideal}), \\ \frac{25}{6} \sqrt{\frac{10}{\pi}} n^{3/2} e^{-5n/2} & (\text{repulsive}), \\ \delta(n-1) & (\text{equidistant}). \end{cases} \quad (17)$$

The bond vector distribution under a given n is simply given as the Gaussian distribution:

$$P_{\text{eq},L}(\mathbf{Q}|n) = \frac{1}{(2\pi n)^{3/2}} e^{-\mathbf{Q}^2/2n}. \quad (18)$$

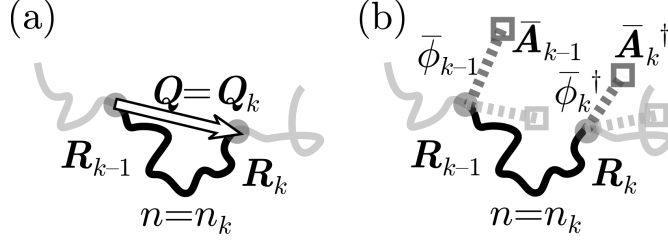


Figure 2: The single-subchain approximation for the single-chain slip-link and slip-spring models. (a) The slip-link model. The statistics of a single subchain (the black solid curve) can be expressed as a function of the bond vector \mathbf{Q} and the segment number n . Other subchains (solid light gray curves) are not explicitly considered. (b) The slip-spring model. The anchoring points and slip-spring size parameters of two slip-springs attached to the tagged subchain are expressed by using effective anchoring points ($\bar{\mathbf{A}}_{k-1}$ and $\bar{\mathbf{A}}_k^\dagger$, gray squares) and effective slip-spring size parameters ($\bar{\phi}_{k-1}$ and $\bar{\phi}_k^\dagger$). The effective anchoring points and slip-spring size parameters are not the same as original anchoring points (light gray circles) and the original slip-spring size parameter.

The joint probability distribution function for the segment number and the bond vector is $P_{\text{eq,L}}(\mathbf{Q}, n) = P_{\text{eq,L}}(\mathbf{Q}|n)P_{\text{eq,L}}(n)$. The bond vector distribution function is calculated as $P_{\text{eq,L}}(\mathbf{Q}) = \int dn P_{\text{eq,L}}(\mathbf{Q}, n)$. The result is:

$$P_{\text{eq,L}}(\mathbf{Q}) = \begin{cases} \frac{1}{2\pi|\mathbf{Q}|} e^{-\sqrt{2}|\mathbf{Q}|} & (\text{ideal}), \\ \frac{25}{6\pi^2} |\mathbf{Q}| K_1(\sqrt{5}|\mathbf{Q}|) & (\text{repulsive}), \\ \frac{1}{(2\pi)^{3/2}} e^{-\mathbf{Q}^2/2} & (\text{equidistant}). \end{cases} \quad (19)$$

Here, $K_1(x)$ is the first order modified Bessel function of the second kind^{26,27}. From the Bayes' theorem, the conditional probability distribution function of n under given \mathbf{Q} is calculated from eqs (17) and (19), as $P_{\text{eq,L}}(n|\mathbf{Q}) = P_{\text{eq,L}}(\mathbf{Q}, n)/P_{\text{eq,L}}(\mathbf{Q})$. Thus we have

$$P_{\text{eq,L}}(n|\mathbf{Q}) = \begin{cases} \frac{1}{\sqrt{2\pi}} \frac{|\mathbf{Q}|}{n^{3/2}} \exp\left(-\frac{\mathbf{Q}^2}{2n} - n + \sqrt{2}|\mathbf{Q}|\right) & (\text{ideal}), \\ \frac{\sqrt{5}}{2} \frac{1}{|\mathbf{Q}| K_1(\sqrt{5}|\mathbf{Q}|)} \exp\left(-\frac{\mathbf{Q}^2}{2n} - \frac{5n}{2}\right) & (\text{repulsive}), \\ \delta(n-1) & (\text{equidistant}). \end{cases} \quad (20)$$

Finally, by using the equilibrium probability distribution functions (19) and (20), the plateau modulus of the single-chain slip-link model becomes

$$\begin{aligned} G_{N,L}^{(0)} &\approx \nu_0 \sum_{Z=1}^{\infty} Z \left[\int d\mathbf{Q} \left[\int dn \frac{1}{n} P_{\text{eq,L}}(n|\mathbf{Q}) \right]^2 Q_x^2 Q_y^2 P_{\text{eq,L}}(\mathbf{Q}) \right] P_{\text{eq,L}}(Z) \\ &= G_0 \int d\mathbf{Q} \left[\int dn \frac{1}{n} P_{\text{eq,L}}(n|\mathbf{Q}) \right]^2 Q_x^2 Q_y^2 P_{\text{eq,L}}(\mathbf{Q}). \end{aligned} \quad (21)$$

Here we have defined the characteristic modulus G_0 as $G_0 \equiv \nu_0 Z_0 = \rho_0$ (This characteristic modulus is common for all the single-chain slip-link and slip-spring models, as shown in Appendix B.) In dimensional units, G_0 is expressed as $G_0 = \nu_0 k_B T N / N_0 = \rho_0 k_B T / N_0$. Therefore, G_0 corresponds to the modulus of an ideal rubber with the average subchain segment number N_0 . In eq (21), the integral over n explicitly depends on the distribution function $P_{\text{eq,L}}(n|\mathbf{Q})$. Therefore, models with different distribution functions have different plateau moduli.

Next we consider the single-chain slip-spring models. In the case of the slip-spring models, we need to specify the anchoring points in addition to the number of segments in the subchain and the bond vector. Under the single-subchain approximation, we cannot simply utilize the anchoring

points and the slip-spring size parameters for the full chain model. The spatial fluctuation of a slip-linked point is affected by two subchains and one slip-spring connected to the point. If we simply cut the subchains connected to a tagged subchain, the fluctuation is affected only by one subchain and one slip-spring. This situation is clearly different from that of the original tagged subchain. To recover the correct fluctuation, we should employ the effective anchoring points and the effective slip-spring size parameters. We consider the k -th subchain as a tagged subchain, as before, and express the effective anchoring points for the $(k-1)$ -th and the k -th anchoring points as $\bar{\mathbf{A}}_{k-1}$ and $\bar{\mathbf{A}}_k^\dagger$, respectively. Also, we express the effective slip-spring size parameters for the $(k-1)$ -th and k -th slip-springs as $\bar{\phi}_{k-1}$ and $\bar{\phi}_k^\dagger$. The schematic image of the single-subchain approximation for the slip-spring model is shown in Figure 2(b). The effective anchoring points and the effective slip-spring size parameters are obtained by integrating-out the degrees of freedom of other subchains. Then we can express the equilibrium probability distribution of a single subchain as $P_{\text{eq,S}}(\mathbf{R}_{k-1}, \mathbf{R}_k, n_k, \{\mathbf{A}_k\})$. Unlike the case of the slip-link model, the bond vector can be equilibrated at the entanglement time scale in the slip-spring model. To calculate the plateau modulus, we consider that the number of segments and the bond vector obey the equilibrium distribution under a given configuration of the anchoring point, $P_{\text{eq,S}}(\mathbf{R}_{k-1}, \mathbf{R}_k, n_k | \{\mathbf{A}_k\})$. We have the following expression for the plateau modulus:

$$G_{N,S}^{(0)} \approx G_0 \int d\{\mathbf{A}_k\} P_{\text{eq,S}}(\{\mathbf{A}_k\}) \left[\int dnd\mathbf{R}_{k-1} d\mathbf{R}_k \frac{Q_{k,x} Q_{k,y}}{n_k} P_{\text{eq,S}}(\mathbf{R}_{k-1}, \mathbf{R}_k, n_k | \{\mathbf{A}_k\}) \right] \\ \times \left[\int dnd\mathbf{R}_{k-1} d\mathbf{R}_k \left[\frac{Q_{k,x} Q_{k,y}}{n_k} + \frac{2(R_{k-1,x} - \bar{A}_{k-1,x})(R_{k-1,y} - \bar{A}_{k-1,y})}{\bar{\phi}_{k-1}} \right. \right. \\ \left. \left. + \frac{2(R_{k,x} - \bar{A}_{k,x}^\dagger)(R_{k,y} - \bar{A}_{k,y}^\dagger)}{\bar{\phi}_k^\dagger} \right] P_{\text{eq,S}}(\mathbf{R}_{k-1}, \mathbf{R}_k, n_k | \{\mathbf{A}_k\}) \right]. \quad (22)$$

To calculate the plateau modulus by eq (22), we should evaluate the integrals over n_k , \mathbf{R}_{k-1} , and \mathbf{R}_k . Unfortunately, even under a single subchain approximation, such integrals cannot be easily evaluated in general. For the equidistant slip-spring model, however, the expression reduces to be simple. Since the number of segments is constant ($n_k = 1$), eq (22) reduces to

$$G_{N,ES}^{(0)} \approx G_0 \int d\{\mathbf{A}_k\} P_{\text{eq,ES}}(\{\mathbf{A}_k\}) \left[\int d\mathbf{R}_{k-1} d\mathbf{R}_k Q_{k,x} Q_{k,y} P_{\text{eq,ES}}(\mathbf{R}_{k-1}, \mathbf{R}_k | \{\mathbf{A}_k\}) \right] \\ \times \left[\int d\mathbf{R}_{k-1} d\mathbf{R}_k \left[Q_{k,x} Q_{k,y} + \frac{(R_{k-1,x} - \bar{A}_{k-1,x})(R_{k-1,y} - \bar{A}_{k-1,y})}{\bar{\phi}_{k-1}} \right. \right. \\ \left. \left. + \frac{(R_{k,x} - \bar{A}_{k,x}^\dagger)(R_{k,y} - \bar{A}_{k,y}^\dagger)}{\bar{\phi}_k^\dagger} \right] P_{\text{eq,ES}}(\mathbf{R}_{k-1}, \mathbf{R}_k | \{\mathbf{A}_k\}) \right]. \quad (23)$$

Here, we note that the equidistant slip-spring model looks similar to the rubber elasticity model by Rubinstein and Panyukov^{28,29}. Eq (23) corresponds to the comb polymer model in the Rubinstein-Panyukov model. For the ideal and repulsive slip-spring models, we employ the decoupling approximation for n_k , and \mathbf{R}_{k-1} and \mathbf{R}_k . Under the decoupling approximation, we calculate the contributions of the integral over n and that over \mathbf{R}_{k-1} and \mathbf{R}_k , separately. The former is the same as the case of the slip-link model, and the latter is the same as the equidistant slip-spring model. Therefore, we have the following approximate expression:

$$\frac{G_{N,S}^{(0)}}{G_0} \approx \frac{G_{N,ES}^{(0)}}{G_0} \frac{G_{N,L}^{(0)}}{G_0}. \quad (24)$$

To obtain the explicit expression of the plateau modulus for the equidistant slip-spring model, we need the equilibrium distribution function for the single subchain with the effective anchoring points and the effective slip-spring sizes. Although the exact expressions become quite complicated,

we can reasonably approximate them by the following forms:

$$\bar{\phi}_{k-1} \approx \bar{\phi}_k^\dagger \approx \bar{\phi}_\infty \equiv \frac{-1 + \sqrt{1 + 4\bar{\phi}}}{2}, \quad (25)$$

$$\bar{\mathbf{A}}_{k-1} \approx \frac{\bar{\phi}_\infty}{\bar{\phi}} \sum_{j=0}^{\infty} \left(1 - \frac{\bar{\phi}_\infty}{\bar{\phi}}\right)^j \mathbf{A}_{k-1-j}, \quad (26)$$

$$\bar{\mathbf{A}}_k^\dagger \approx \frac{\bar{\phi}_\infty}{\bar{\phi}} \sum_{j=0}^{\infty} \left(1 - \frac{\bar{\phi}_\infty}{\bar{\phi}}\right)^j \mathbf{A}_{k+j}. \quad (27)$$

The detailed derivations of eqs (25)-(27) are shown in Appendix C. With the effective anchoring points and the effective slip-spring size parameters by eqs (25)-(27), the equilibrium distribution function for the single subchain becomes

$$P_{\text{eq,ES}}(\mathbf{R}_{k-1}, \mathbf{R}_k | \{\mathbf{A}_k\}) = \frac{(1 + 2\bar{\phi}_\infty)^{3/2}}{(2\pi\bar{\phi}_\infty)^3} \exp \left[-\frac{(\mathbf{R}_k - \mathbf{R}_{k-1})^2}{2} - \frac{(\mathbf{R}_{k-1} - \bar{\mathbf{A}}_{k-1})^2}{2\bar{\phi}_\infty} \right. \\ \left. - \frac{(\mathbf{R}_k - \bar{\mathbf{A}}_k^\dagger)^2}{2\bar{\phi}_\infty} + \frac{(\bar{\mathbf{A}}_k - \bar{\mathbf{A}}_k^\dagger)^2}{1 + 2\bar{\phi}_\infty} \right]. \quad (28)$$

3.2 Slip-Link Models

We calculate the plateau moduli of the single-chain slip-link models. The simplest case is the equidistant slip-link model. In the case of the equidistant slip-link model, from eq (20), the integral in eq (21) is trivial:

$$\int dn \frac{1}{n} P_{\text{eq,EL}}(n | \mathbf{Q}) = 1. \quad (29)$$

Then we have the following explicit form for the plateau modulus:

$$\frac{G_{N,\text{EL}}^{(0)}}{G_0} \approx \int d\mathbf{Q} Q_x^2 Q_y^2 P_{\text{eq,EL}}(\mathbf{Q}) = 1. \quad (30)$$

The equidistant slip-link model has no fluctuation and thus this result is physically reasonable. Roughly speaking, this result corresponds to the pure reptation model (without the relaxation by the longitudinal motion).

For the ideal or repulsive slip-link models, explicit expressions for the integral in eq (21) become a bit complicated. For the ideal slip-link model, we have

$$\int dn \frac{1}{n} P_{\text{eq,IL}}(n | \mathbf{Q}) = \int_0^\infty dn \frac{1}{n} \frac{1}{\sqrt{2\pi}} \frac{|\mathbf{Q}|}{n^{3/2}} \exp \left(-\frac{Q^2}{2n} - n + \sqrt{2}|\mathbf{Q}| \right) \\ = \frac{1}{Q^2} + \frac{\sqrt{2}}{|\mathbf{Q}|}, \quad (31)$$

and thus the plateau modulus is approximately expressed as

$$\frac{G_{N,\text{IL}}^{(0)}}{G_0} \approx \int d\mathbf{Q} \left(\frac{1}{Q^2} + \frac{\sqrt{2}}{|\mathbf{Q}|} \right)^2 Q_x^2 Q_y^2 P_{\text{eq,IL}}(\mathbf{Q}). \quad (32)$$

The integral over \mathbf{Q} can be simplified by using the polar coordinates, ($Q_x = Q \cos \theta \cos \varphi$, $Q_y = Q \cos \theta \sin \varphi$, and $Q_z = Q \sin \theta$):

$$\frac{G_{N,\text{IL}}^{(0)}}{G_0} \approx \int_0^\infty dQ \int_0^{2\pi} d\theta \int_{-\pi/2}^{\pi/2} d\varphi Q^2 \cos \varphi \left[(1 + \sqrt{2}Q)^2 \cos^4 \varphi \sin^2 \theta \cos^2 \theta \right] \frac{1}{2\pi Q} e^{-\sqrt{2}Q} \\ = \frac{2}{15} \int_0^\infty dQ [Q + 2\sqrt{2}Q^2 + 2Q^3] e^{-\sqrt{2}Q} = \frac{11}{15}. \quad (33)$$

Then we have the following simple expression for the plateau modulus of the ideal slip-link model:

$$\frac{G_{N,IL}^{(0)}}{G_0} = \frac{11}{15} \approx 0.7333. \quad (34)$$

Unlike the case of the equidistant slip-link model, the plateau modulus of the ideal slip-link model is lower than the characteristic modulus G_0 . This can be interpreted as the effect of the fluctuation of the segment number.

We consider the repulsive slip-link model. This model has probability distributions less simpler than other slip-link models. The integral in eq (21) becomes

$$\begin{aligned} \int dn \frac{1}{n} P_{\text{eq,RL}}(n|\mathbf{Q}) &= \frac{\sqrt{5}}{2} \frac{1}{|\mathbf{Q}| K_1(\sqrt{5}|\mathbf{Q}|)} \int_0^\infty dn \frac{1}{n} \exp\left(-\frac{Q^2}{2n} - \frac{5n}{2}\right) \\ &= -\frac{2}{|\mathbf{Q}| K_1(\sqrt{5}|\mathbf{Q}|)} \frac{\partial}{\partial(Q^2)} \left[|\mathbf{Q}| K_1(\sqrt{5}|\mathbf{Q}|) \right] \\ &= \frac{\sqrt{5} K_0(\sqrt{5}|\mathbf{Q}|)}{|\mathbf{Q}| K_1(\sqrt{5}|\mathbf{Q}|)}. \end{aligned} \quad (35)$$

As the case of the ideal slip-link model, the polar coordinates are convenient to calculate the plateau modulus. The plateau modulus becomes

$$\begin{aligned} \frac{G_{N,RL}^{(0)}}{G_0} &\approx \int d\mathbf{Q} \left[\frac{\sqrt{5} K_0(\sqrt{5}|\mathbf{Q}|)}{|\mathbf{Q}| K_1(\sqrt{5}|\mathbf{Q}|)} \right]^2 Q_x^2 Q_y^2 P_{\text{eq,RL}}(\mathbf{Q}) \\ &= \frac{1}{6\pi^2} \int_0^\infty d\zeta \int_0^\infty d\theta \int_{-\pi/2}^{\pi/2} d\varphi \frac{K_0^2(\zeta)}{K_1(\zeta)} \zeta^5 \cos^5 \varphi \cos^2 \theta \sin^2 \theta \\ &= \frac{2}{45\pi} \int_0^\infty d\zeta \zeta^5 \frac{K_0^2(\zeta)}{K_1(\zeta)}, \end{aligned} \quad (36)$$

where we have set $\zeta = \sqrt{5}|\mathbf{Q}|$. By numerically evaluating the integral over ζ , we have the following expression for the plateau modulus for the repulsive slip-link model:

$$\frac{G_{N,RL}^{(0)}}{G_0} \approx 0.8214. \quad (37)$$

Thus we find that the plateau modulus of the repulsive slip-link model is smaller than that of the equidistant model yet is larger than that of the ideal slip-link model. The fluctuation of the segment number in the repulsive slip-link model is relatively suppressed (by the repulsive interaction), and thus the resulting plateau modulus becomes larger than that of the ideal slip-link model.

3.3 Slip-Spring Models

As we mentioned, we calculate the plateau modulus of the slip-spring models by utilizing the decoupling approximation (eq (24)). Therefore, what we need to calculate here is the plateau modulus of the equidistant slip-spring model by eq (23). The integrals over \mathbf{R}_{k-1} and \mathbf{R}_k in eq (23) become as follows:

$$\begin{aligned} &\int d\mathbf{R}_{k-1} d\mathbf{R}_k Q_{k,x} Q_{k,y} P_{\text{eq,ES}}(\mathbf{R}_{k-1}, \mathbf{R}_k | \{\mathbf{A}_k\}) \\ &= \frac{(\bar{A}_{k,x}^\dagger - \bar{A}_{k-1,x})(\bar{A}_{k,y}^\dagger - \bar{A}_{k-1,y})}{(1 + 2\bar{\phi}_\infty)^2}, \end{aligned} \quad (38)$$

$$\begin{aligned}
& \int d\mathbf{R}_{k-1} d\mathbf{R}_k \frac{(R_{k-1,x} - \bar{A}_{k-1,x})(R_{k-1,y} - \bar{A}_{k-1,y})}{\bar{\phi}_\infty} P_{\text{eq,ES}}(\mathbf{R}_{k-1}, \mathbf{R}_k | \{\mathbf{A}_k\}) \\
&= \int d\mathbf{R}_{k-1} d\mathbf{R}_k \frac{(R_{k,x} - \bar{A}_{k,x}^\dagger)(R_{k,y} - \bar{A}_{k,y}^\dagger)}{\bar{\phi}_\infty} P_{\text{eq,ES}}(\mathbf{R}_{k-1}, \mathbf{R}_k | \{\mathbf{A}_k\}) \\
&= \frac{\bar{\phi}_\infty (\bar{A}_{k,x}^\dagger - \bar{A}_{k-1,x})(\bar{A}_{k,y}^\dagger - \bar{A}_{k-1,y})}{(1 + 2\bar{\phi}_\infty)^2}.
\end{aligned} \tag{39}$$

Then eq (23) can be rewritten in a simple form as

$$\begin{aligned}
\frac{G_{N,\text{ES}}^{(0)}}{G_0} &\approx \frac{1}{(1 + 2\bar{\phi}_\infty)^3} \sum_{j,k=1}^{Z_0} \int d\{\mathbf{A}_k\} (\bar{A}_{k,x}^\dagger - \bar{A}_{k-1,x})^2 (\bar{A}_{k,y}^\dagger - \bar{A}_{k-1,y})^2 P_{\text{eq,ES}}(\{\mathbf{A}_k\}) \\
&= \frac{1}{(1 + 2\bar{\phi}_\infty)^3} \langle (\bar{A}_{k,x}^\dagger - \bar{A}_{k-1,x})^2 \rangle_{\text{eq}}.
\end{aligned} \tag{40}$$

Thus we find that we can calculate the plateau modulus of the equidistant slip-spring model once the explicit expression for the variance for $\bar{A}_{k,x}^\dagger - \bar{A}_{k-1,x}$ is obtained.

The vector $\bar{\mathbf{A}}_k^\dagger - \bar{\mathbf{A}}_k$ can be rewritten in terms of the bond vector for the anchoring point, $\mathbf{U}_k \equiv \mathbf{A}_k - \mathbf{A}_{k-1}$, as

$$\begin{aligned}
\bar{\mathbf{A}}_k^\dagger - \bar{\mathbf{A}}_{k-1} &= \frac{\bar{\phi}_\infty}{\phi} \sum_{j=0}^{\infty} \left(1 - \frac{\bar{\phi}_\infty}{\phi}\right)^j (\mathbf{A}_{k+j} - \mathbf{A}_{k-1-j}) \\
&= \frac{\bar{\phi}_\infty}{\phi} \sum_{j=0}^{\infty} \left(1 - \frac{\bar{\phi}_\infty}{\phi}\right)^j (\mathbf{U}_{k+j} + \cdots + \mathbf{U}_{k-j}) \\
&= \sum_{j=-\infty}^{\infty} \left(1 - \frac{\bar{\phi}_\infty}{\phi}\right)^{|j|} \mathbf{U}_{k+j}.
\end{aligned} \tag{41}$$

The bond vectors $\{\mathbf{U}_k\}$ obey the Gaussian distribution, and the mean and variance are given as

$$\langle \mathbf{U}_k \rangle_{\text{eq}} = 0, \quad \langle \mathbf{U}_k \mathbf{U}_j \rangle_{\text{eq}} = \begin{cases} (1 + 2\phi) \mathbf{1} & (k = j), \\ -\phi \mathbf{1} & (k = j \pm 1), \\ 0 & (\text{otherwise}). \end{cases} \tag{42}$$

Here, $\mathbf{1}$ represents the unit tensor. The detailed calculations are shown in Appendix C. From eqs (41) and (42), the variance of $\bar{A}_{k,x}^\dagger - \bar{A}_{k-1,x}$ is calculated to be

$$\begin{aligned}
\langle (\bar{A}_{k,x}^\dagger - \bar{A}_{k-1,x})^2 \rangle_{\text{eq}} &= \sum_{j,l=-\infty}^{\infty} \left(1 - \frac{\bar{\phi}_\infty}{\phi}\right)^{|j|+|l|} \langle U_{k+j,x} U_{k+l,x} \rangle_{\text{eq}} \\
&= \sum_{j=-\infty}^{\infty} \left[(1 + 2\phi) \left(1 - \frac{\bar{\phi}_\infty}{\phi}\right)^{2|j|} - 2\phi \left(1 - \frac{\bar{\phi}_\infty}{\phi}\right)^{|j|+|j+1|} \right] \\
&= \frac{2(1 + 2\phi)}{1 - (1 - \bar{\phi}_\infty/\phi)^2} - (1 + 2\phi) - \frac{4\phi(1 - \bar{\phi}_\infty/\phi)}{1 - (1 - \bar{\phi}_\infty/\phi)^2} \\
&= 1 + 2\bar{\phi}_\infty.
\end{aligned} \tag{43}$$

Finally we have the following simple expression for the plateau modulus of the equidistant slip-spring model:

$$\frac{G_{N,\text{ES}}^{(0)}}{G_0} \approx \frac{1}{1 + 2\bar{\phi}_\infty} = \frac{1}{\sqrt{1 + 4\phi}}. \tag{44}$$

As the slip-spring size parameter ϕ increases, the plateau modulus decreases. If the slip-spring size parameter is sufficiently small, a slip-spring behaves as a slip-link. At the limit of $\phi \rightarrow 0$,

the fluctuation of the bond vanishes and the plateau modulus of the equidistant slip-link model is recovered. (This limit would be interpreted as the pure reptation model.) It would be fair to mention that Rubinstein and Panyukov²⁸ obtained a similar factor by a slightly different calculation. From eq (44), the plateau moduli for the ideal and equidistant slip-springs are roughly estimated as

$$\frac{G_{N,IS}^{(0)}}{G_0} \approx \frac{11/15}{\sqrt{1+4\phi}}, \quad \frac{G_{N,RS}^{(0)}}{G_0} \approx \frac{0.8214}{\sqrt{1+4\phi}}. \quad (45)$$

Eqs (44) and (45) are the main results of this work. The ratio of the plateau modulus to G_0 depends both on the interaction between slip-links and the slip-spring size parameter ϕ .

4 Simulation

Although we obtained the analytic expressions for the plateau modulus in the previous section (eqs (44) and (45)), they are based on the single-subchain approximation and the decoupling approximation. Under the single-subchain approximation, correlations between different subchains are ignored and thus the results would not be accurate. Also, the decoupling approximation is generally not so accurate. To check the accuracy of our theory, in this section we perform single-chain simulations without these approximations. Then we can directly evaluate the plateau moduli with eqs (11) and (16).

As we mentioned, there are various similar but different slip-link and slip-spring type models. Here we limit ourselves to simple models, and do not directly compare elaborated simulation models. We employ the single-chain slip-link and slip-spring models (without single-subchain approximations) as simulation models. The comparison with the literature data by some elaborated simulation models are shown in Section 5.1.

Here we describe the simulation scheme. First we generate a polymer chain with slip-linked points by the equilibrium probability distribution. We assume that the average number of slip-links (or slip-springs) Z_0 is sufficiently large. Then we can use the segment number distribution for a single subchain as a very accurate approximation. The algorithm to generate a slip-linked or slip-springed chain is as follows.

1. Set the segment index $s = 0$ and the subchain index $k = 1$.
2. Generate n_k from the equilibrium distribution of the segment number distribution (eq (17)).
3. If $s + n_k < Z_0$, increase s and k as $s \rightarrow s + n_k$ and $k \rightarrow k + 1$, and then go to the step 2.
4. Set $Z = k$ and $n_Z = Z_0 - s$.
5. Set $\mathbf{R}_0 = 0$.
6. For $k = 1, 2, \dots, Z$, generate the slip-linked or slip-springed positions \mathbf{R}_k from the Gaussian distribution.
7. For slip-springed chains, generate the anchoring points \mathbf{A}_k ($k = 0, 1, \dots, Z$) from the Gaussian distribution.

To obtain the locally equilibrated state after τ_e , we evolve the system by the Monte Carlo method. For the ideal and repulsive models, the segment numbers $\{n_k\}$ are equilibrated. (In the equidistant slip-link and slip-spring models, the segment number in a subchain is constant and thus this exchange is not performed.) We employ the Metropolis type acceptance and rejection probabilities. The equilibration scheme is as follows.

1. Randomly choose two subchains indices j and k .
2. Randomly sample the number of segments Δn to be exchanged, from the uniform distribution. Δn is uniformly distributed in the range

$$-n_j \leq \Delta n \leq n_k, \quad (46)$$

to avoid n_j or n_k being negative.

3. Accept the exchange by the following probability:

$$P(n_j + \Delta n, n_k - \Delta n | n_j, n_k) = \min \left\{ 1, e^{-\Delta \mathcal{F}(j,k;\Delta n)} \right\}. \quad (47)$$

where the free energy difference $\Delta \mathcal{F}(j, k; \Delta n)$ is given as

$$\Delta \mathcal{F}_I(j, k; \Delta n) \equiv \frac{\Delta n}{2} \left[\frac{(\mathbf{R}_k - \mathbf{R}_{k-1})^2}{n_k(n_k - \Delta n)} - \frac{(\mathbf{R}_j - \mathbf{R}_{j-1})^2}{n_j(n_j + \Delta n)} \right] + \frac{3}{2} \ln \frac{(n_j + \Delta n)(n_k - \Delta n)}{n_j n_k}, \quad (48)$$

$$\Delta \mathcal{F}_R(j, k; \Delta n) \equiv \frac{\Delta n}{2} \left[\frac{(\mathbf{R}_k - \mathbf{R}_{k-1})^2}{n_k(n_k - \Delta n)} - \frac{(\mathbf{R}_j - \mathbf{R}_{j-1})^2}{n_j(n_j + \Delta n)} \right], \quad (49)$$

for the ideal (“I”) and repulsive (“R”) models, respectively.

For slip-spring models, the positions of slip-springed points $\{\mathbf{R}_k\}$ are also equilibrated. We randomly select one bead j and then resample \mathbf{R}_j from the local equilibrium distribution. Because the subchains and slip-springs are linear springs, the local equilibrium distribution of \mathbf{R}_j becomes the Gaussian. The resampling scheme is as follows.

1. Randomly select the index j .
2. Sample the Gaussian random number vector \mathbf{w} from the standard normal distribution. The first and second statistical moments of \mathbf{w} are given as $\langle \mathbf{w} \rangle = 0$ and $\langle \mathbf{w} \mathbf{w} \rangle = \mathbf{1}$.
3. Generate the new position of the j -th point \mathbf{R}_j as

$$\mathbf{R}_j \rightarrow \begin{cases} \frac{n_j^{-1} \mathbf{R}_{j-1} + n_{j+1}^{-1} \mathbf{R}_{j+1} + \phi^{-1} \mathbf{A}_j}{n_j^{-1} + n_{j+1}^{-1} + \phi^{-1}} + (n_j^{-1} + n_{j+1}^{-1} + \phi^{-1})^{-1/2} \mathbf{w} & (1 \leq j \leq Z), \\ \frac{n_1^{-1} \mathbf{R}_1 + \phi^{-1} \mathbf{A}_0}{n_1^{-1} + \phi^{-1}} + (n_1^{-1} + \phi^{-1})^{-1/2} \mathbf{w} & (j = 0), \\ \frac{n_Z^{-1} \mathbf{R}_{Z-1} + \phi^{-1} \mathbf{A}_Z}{n_Z^{-1} + \phi^{-1}} + (n_Z^{-1} + \phi^{-1})^{-1/2} \mathbf{w} & (j = Z). \end{cases} \quad (50)$$

After sufficient Monte Carlo trials (the total number of trials should be sufficiently large so that the local equilibrium state is realized), we calculate the product of the stress tensors appearing in eq (13) (for slip-link models) or in eq (16) (for slip-spring models). Finally, by taking the average over different samples (different random number sequences), we have the plateau modulus.

We use the Mersenne Twister random number generator³⁰ to generate random numbers. We also use the standard Box-Muller method³¹ and the Marsaglia-Tsang method³² to generate random numbers which obey the normal and gamma distributions, respectively. In this work, we set the number of average subchains as $Z_0 = 100$, the total number of Monte Carlo trials as $N_{\text{MC}} = 10^3 Z_0$, and the number of samples (chains) as $N_{\text{samples}} = 10^5$. (The simulation results are not sensitive to these parameters, as far as they are sufficiently large.)

The Monte Carlo simulation data and theoretical predictions are shown in Figure 3. $\phi = 0$ corresponds to the slip-link model. For the equidistant slip-spring model, the theoretical curve coincides to the simulation data almost perfectly. For the repulsive and ideal slip-spring models, the theoretical curves slightly deviate from the simulation data in the relatively large ϕ region. For the slip-link models ($\phi = 0$), the agreement between the theoretical prediction and the simulation data is very good. The deviation becomes larger as the slip-spring size parameter ϕ increases, but even for relatively high ϕ , the deviation is not so large. This result means that the single-subchain approximation is accurate for the slip-link and slip-spring models. The deviation would be due to the coupling of the fluctuations for the segment number and the bond vector. (Judging from the simulation data, the decoupling approximation slightly overestimates the fluctuations.)

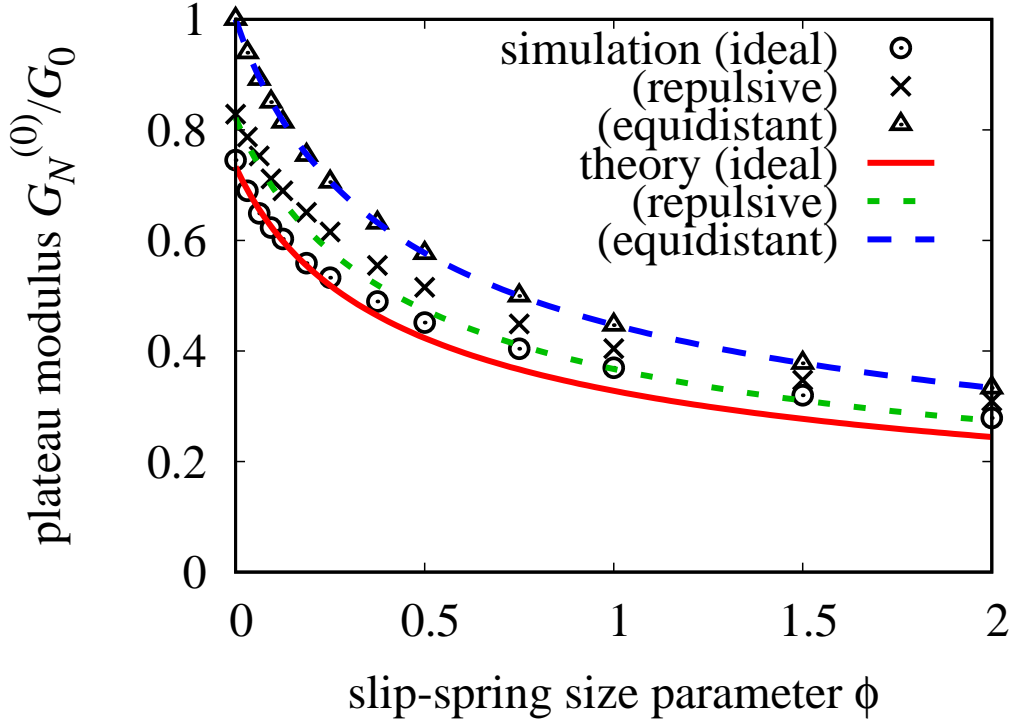


Figure 3: Plateau moduli of several single-chain slip-link and slip-spring models. Symbols show simulation data by the Monte Carlo method, and curves show theoretical predictions (eqs (44) and (45)). The slip-link models correspond to the slip-spring models with the slip-spring size parameter $\phi = N_s/N_0 = 0$.

5 Discussions

5.1 Comparison with Simulation Data

Here we compare our simulation results with literature data by some slip-link and slip-spring models. Masubuchi et al⁸ performed PCN simulations (the statistics of their model is similar to the repulsive slip-link model), and reported that the plateau modulus is given by $G_N^{(0)} = (4/5)G_0$ if slip-linked points are fixed in space and only the segment numbers are allowed to be equilibrated. (Although the PCN model is a multi-chain slip-link model, this result corresponds to the single-chain model because slip-linked points are fixed and intrachain correlation is negligible.) Nair and Schieber¹⁵ reported that N_0 is well estimated from $G_N^{(0)}$ via $G_N^{(0)} = (4/5)G_0$ for their slip-link model (which corresponds to the ideal slip-link model in this work). Although these results do not perfectly agree with our theory and Monte Carlo simulation data, the decrease of the plateau modulus by the factor $4/5 = 0.8$ is close to our result ($G_N^{(0)}/G_0 = 0.7333$ or 0.8214). (Strictly speaking, the plateau modulus at $t \approx \tau_e$ in the PCN model⁸ seems to be slightly larger than 0.8. This is consistent with our prediction.) For the slip-spring model, the ideal single-chain slip-spring simulations with $N_0 = 4$ and $N_s = 0.5$ ($\phi = 0.125$) give roughly $G_N^{(0)}/G_0 \approx 0.4$.^{14,25} Our theory and the Monte Carlo simulation result give $G_N^{(0)}/G_0 \approx 0.60$. This value is somewhat larger than the simulation result. However, the estimate of the plateau modulus from the simulation data involves some errors, and we consider the agreement is not that bad. For the ideal slip-spring model, Likhtman¹⁴ examined the effects of N_0 and N_s on the plateau modulus, and reported some combinations of N_0 and N_s which give almost the same plateau modulus; $(N_0, N_s) = (1, 4), (2, 1.75)$, and $(4, 0.5)$. These parameter sets give the slip-spring size parameters as $\phi = 4, 0.875$, and 0.125 , respectively. Our theory predicts the plateau moduli for these parameter

sets as $G_N^{(0)}/\rho_0 k_B T \approx 0.18, 0.17$, and 0.15 , respectively, and these values are reasonably close to each other. (Note that here we have normalized $G_N^{(0)}$ by $\rho_0 k_B T$ instead of $G_0 = \rho_0 k_B T/N_0$. The value of $G_N^{(0)}/G_0$ strongly depends on ϕ .) Judging from these results, we consider that our theory is reasonable to estimate the plateau moduli of various slip-link and slip-spring models.

Even if our theory works well, we should note that the comparison shown above was done for the single-chain models. In reality, the entanglement originates from the non-crossability of polymer chains, and the validity of the single-chain models is not guaranteed *a priori*. The relations between the multi-chain slip-link and slip-spring models and the corresponding single-chain models are not clear. Naively, we expect that the fluctuations of slip-linked or slip-springed points in multi-chain models are stronger than those of single-chain models. We consider that such fluctuations are similar to those in cross-linked networks. For the case of cross-linked networks, the shear modulus of a network can be related to the fluctuations of cross-linked points⁷. For the ideal phantom f -functional random network, the shear modulus G can be expressed as

$$G = (1 - 2/f)\nu_0 k_B T \quad (51)$$

where ν_0 is the average subchain number density. Everaers³³ analyzed series of network structures in molecular dynamics simulations extracted by primitive path analyses, and reported that the plateau moduli can be well reproduced by eq (51) with $f = 4$. If we assume that the similar expression holds for the multi-chain slip-link models, the plateau modulus is reduced by the factor $(1 - 2/f)$ from the prediction for the single-chain slip-spring model. At the single-chain level, this reduction would be re-interpreted as the fluctuation of the slip-spring. As we mentioned, we expect that slip-spring models can reproduce some of the fluctuation effects. The degree of the fluctuation depends on the slip-spring size parameter ϕ in the slip-spring model whereas it depends on the functionality f in the phantom network model. Then we may simply employ the following relation: $1/\sqrt{1+4\phi} \approx 1 - 2/f$, which gives $\phi \approx (f-1)/(f-2)^2$. For tri- and tetra-functional networks ($f = 3$ and 4), we have $\phi \approx 2$ and $3/4$, respectively. With this interpretation, the PCN model corresponds to the repulsive slip-spring model with $f = 4$, and thus our theory predicts $G_N^{(0)}/G_0 \approx 0.41$. This estimate seems to be consistent with the PCN simulation data.⁸ The multi-chain slip-spring (MCSS) model¹⁷ corresponds to the ideal slip-spring model with $f = 3$, and our theory predicts $G_N^{(0)}/G_0 \approx 0.24$. This value seems to be somewhat larger than the simulation data ($G_N^{(0)}/G_0 \approx 0.17$) yet still not that bad.

Recently, the detailed comparison among the molecular dynamics model, the PCN model, and the MCSS model was reported⁶. The relation between the plateau moduli was shown to be $(G_{N,\text{PCN}}^{(0)}/G_0)/(G_{N,\text{MCSS}}^{(0)}/G_0) = 3.2$. This value is also somewhat larger than the prediction by our theory, $0.41/0.24 = 1.7$. For the MCSS model, our theory seems to overestimate the plateau modulus. There are several possible reasons for this. In the MCSS model, two ends of a slip-spring can be attached to the same polymer chain. Then, for some conformations, slip-springs and some subchains may not contribute to the stress. Such slip-springs and subchains decrease the stress compared with a naive estimate. Also, the motion of slip-springs is rather strongly coupled to the motion of polymer chains. The coupling between different fluctuation mechanisms may enhance the fluctuations, and the fluctuations in the MCSS model may be larger than our estimate. (According to the simulation data with different effective fugacities, the values of $G_{N,\text{MCSS}}^{(0)}/G_0$ are approximately constant and thus independent of the effective fugacity³⁴. Thus the fluctuation mechanisms in the MCSS would not be sensitive to parameters in the MCSS model.)

The value of $G_N^{(0)}/G_0$ for each model can be also estimated by fitting the simulation data to experimental data^{5,35,36}. In the case of the PCN model, the fitting gives $G_N^{(0)}/G_0 \approx 0.6$ ⁵. This value is larger than the estimate based only on the simulation data, and is also larger than our theoretical prediction. In the case of the MCSS model, the fitting to experimental data gives $G_N^{(0)}/G_0 \approx 0.3$. With these values we have $(G_{N,\text{PCN}}^{(0)}/G_0)/(G_{N,\text{MCSS}}^{(0)}/G_0) = 2$, which seems to be close to the theoretical prediction. However, it would be fair to mention that the fitting processes usually involve some errors and uncertainties, and the estimated values depend on the details of the analysis and fitting methods. We expect that our theoretical results work as reasonable estimates for $G_N^{(0)}/G_0$ in various slip-link and slip-spring models, within a certain error range.

Our result suggests that the average number of segments between slip-links (or slip-springs), or other similar quantities which characterizes the topological constraints, can *not* be calculated only from the plateau modulus (unless the detailed fluctuation mechanism of the model is fully known). The plateau moduli of slip-link and slip-spring models are smaller than the modulus of the ideal rubber network with the average segment number N_0 , unless the fluctuations are totally suppressed by such as the strong repulsive potential. If we define the entanglement segment number N_e by eq (2), $N_e/N_0 = G_0/G_N^{(0)}$ and thus N_e is larger than N_0 . As we showed, the ratio $G_N^{(0)}/G_0$ is a model-dependent quantity, and therefore N_e/N_0 is also model-dependent. Especially, in reality, there are no slip-links nor slip-springs in entangled polymeric systems, and thus the model-specific interpretation of the plateau modulus may lead physically incorrect conclusions. We should be careful to calculate or estimate N_0 from experimental linear viscoelasticity data.

In recent years, the entanglement segment number and related physical quantities are widely studied by the primitive path analyses^{37–40}. Although there are several different primitive path analysis methods, the central idea is common. The primitive paths can be extracted by virtually fixing the chain ends and stretching chains tightly. Then, from the thus obtained primitive paths, some statistical quantities such as the average contour length and the statistical distribution of the topological constraints can be directly calculated. We can estimate the entanglement segment number by the primitive path, N_{PP} , from these quantities. The primitive path analyses have been applied for various molecular models such as the atomistic and coarse-grained Kremer-Grest molecular dynamics models. The entanglement segment number from the primitive path, N_{PP} , seems to be smaller than that calculated from the plateau modulus, N_e . Everaers³³ collected the literature data and calculated N_{PP}/N_e for various molecular models with various primitive path analysis methods. According to his data, N_{PP}/N_e seems to be roughly about 0.5. However, the reported values of N_{PP}/N_e are not exactly the same value but seem to depend on the details of the analysis method and the system. Therefore, we consider that N_{PP} is rather similar to N_0 in slip-link and slip-spring models. The difference among different primitive path extraction methods may result in different statistical properties. We expect that, as the case of the slip-link and slip-spring models, the ratio N_{PP}/N_e would reflect something like fluctuations. The ratio N_{PP}/N_e would be an important quantity when we compare the coarse-grained models and molecular dynamics simulations. Steenbakkers et al⁴ proposed a method to map the primitive path to the single-chain slip-link model. Recent work by Becerra et al⁴¹ showed that an atomistic molecular model for polyethylene oxide (PEO) can be quantitatively mapped onto some single-chain slip-link models. Although they showed good agreement between experimental and simulation relaxation modulus data, whether their method works well for other systems such as the slip-spring model is not clear. To realize such a mapping, we should understand statistical properties of target models in detail. Our results may be utilized to develop similar mapping method for various slip-link and slip-spring models.

5.2 Relaxation by Longitudinal Motion

In our theory, the effect of the longitudinal motion¹ is not taken into account. This is because at the time scale of $t \approx \tau_e$, the longitudinal motion cannot occur. (Sometimes the relaxation motion of the longitudinal motion is also referred as the contour length fluctuation (CLF). Here, to make the relaxation mechanism clear, we use the term longitudinal motion.) However, the reduction of the stress by the longitudinal motion is widely employed in the analyses for the plateau modulus. According to the standard tube theory, the plateau modulus is modulated from the classical formula and given as¹

$$G_N^{(0)} = \frac{4}{5} \frac{\rho_0 k_B T}{N'_e}. \quad (52)$$

Here, N'_e represents the characteristic segment number which characterizes the tube segment size. (We note that eq (52) was calculated essentially in the same way as eq (1).⁴²) If the longitudinal motion is absent, the plateau modulus becomes $G_N^{(0)} = \rho_0 k_B T / N'_e$ (the characteristic segment number N'_e is assumed to be the same as that in eq (52)). Thus the longitudinal motion reduces the plateau modulus by the factor 4/5, in a similar way to the fluctuations of segment numbers

and slip-springed points in our model. Likhtman and McLeish⁹ analyzed the longitudinal modes of a polymer chain in a tube in detail, and showed that the longitudinal motion does not give the decrease of the plateau modulus at the time scale $t \lesssim \tau_e$. This is physically natural because the characteristic time scale for the relaxation of the longitudinal modes is τ_R . (Their analysis is based on the tube model and thus it may not be fully applicable to the slip-link and slip-spring models. However, the characteristic time scale of the longitudinal modes is common for other models.) Therefore, from the view point of the time scale, the theoretical validity of eq (52) is somewhat questionable.

Our analysis showed that the decrease of the plateau modulus is caused by the fluctuations (or relaxation) of segment numbers and slip-springed points, which occur at the short time scale. Thus our result is not inconsistent with the Likhtman and McLeish's analysis. (Roughly speaking, the tube model can be interpreted as the equidistant slip-link model in which the plateau modulus is simply given as G_0 .) As we mentioned, our theory predicts the numerical factor 0.7333 or 0.8214 at the time scale of $t \approx \tau_e$. These factors are close to $4/5$. In addition, if we tune the repulsive interaction between slip-links precisely, we may be able to perfectly reproduce the factor $4/5$.

Therefore, it would be dangerous to blindly employ eq (52). The segment number between entanglements is sometimes estimated as N'_e by utilizing eq (52) (so-called the Graessley type definition)^{43,10}:

$$N'_e = \frac{4}{5} \frac{\rho_0 k_B T}{G_N^{(0)}} = \frac{4}{5} N_e, \quad (53)$$

However, according to the discussions above, this seems not to be sound. The definition of the segment number between entanglements should not depend on a specific theoretical interpretation⁴⁴. If we employ eq (53) as the definition of the segment number between entanglement instead of N_e by eq (2), the physical interpretation of the segment number between entanglements becomes rather complicated. (We will need to introduce an extra numerical factor $5/4$ to relate N_0 to this segment number between entanglement N'_e .) Based on the results shown above, we conclude that the classical and traditional definition by eq (2) should be employed for the segment number between entanglements. The relaxation mechanisms which have longer time scales than τ_e should not be considered when we study the properties of the plateau modulus.

6 Conclusions

We theoretically calculated the plateau moduli of the single-chain slip-link and slip-spring models. We employed several approximations such as the single-subchain approximation and the decoupling approximation, to analytically calculate the plateau moduli. We showed that the plateau modulus depends on various factors such as the interaction between slip-links and the spring constant of a slip-spring. The plateau modulus increases as the repulsive interaction between slip-links or slip-springs increases. Also, the plateau modulus decreases as the slip-spring size parameter increases. We obtained quantitative predictions which relate parameters in slip-link and slip-spring models to the plateau modulus.

We compared our theoretical results (eqs (44) and (45)) with the Monte Carlo simulation results and the simulation data in the literature. The agreement between theoretical results and Monte Carlo simulation results is good. Our theory slightly underestimates the plateau moduli when the slip-spring size parameter is large. From the comparison of the theoretical results and the literature data, we found that our theory can roughly explain the simulation data (although the agreement is not perfect). Conventionally, the reduction of the plateau modulus is mainly interpreted as the effect of the longitudinal motion. Our theory gives a new and physically reasonable interpretation for the reduction of the plateau modulus.

From the results of this work, we conclude that the segment number between entanglements N_e and the segment number between two slip-links or slip-springs N_0 are generally different and the relation between them is model-dependent. We consider that this work justifies to use N_0 and N_e (or $G_N^{(0)}$) as independent fitting parameters for slip-link and slip-spring models. The ratio N_0/N_e reflects short time fluctuation mechanisms, and thus it is strongly model-dependent. This ratio

would be useful when we compare several different entanglement models and check the consistency among them. It would be also useful to map one simulation model to another simulation model and perform multi-scale simulations.

Acknowledgment

This work was supported by Grant-in-Aid (KAKENHI) for Scientific Research Grant B Number JP19H01861, Grant-in-Aid (KAKENHI) for Scientific Research on Innovative Areas “Discrete Geometric Analysis for Materials Design” Grant Number JP20H04636 (from Ministry of Education, Culture, Sports, Science, and Technology), JST-PRESTO Grant Number JPMJPR1992, and JST-CREST Grant Number JPMJCR1992 (from Japan Science and Technology Agency).

Appendix

A Simple Derivation of Equilibrium Probability Distributions for Single Subchain

In this appendix, we derive equilibrium probability distribution functions for a single subchain in the single-chain slip-link models. Following the idea by Greco⁴⁵, we introduce the effective chemical potential to control the number of segments in a subchain. Then we can directly calculate the statistical properties of a single subchain. We employ the same dimensionless units in the main text. The joint probability distribution of the segment number n and the bond vector \mathbf{Q} for a subchain is given as:

$$P_{\text{eq}}(\mathbf{Q}, n) \propto e^{-\mathcal{F}_{\text{single}}(\mathbf{Q}, n) - \mu n}, \quad (54)$$

where $\mathcal{F}_{\text{single}}(\mathbf{Q}, n)$ is the free energy for a single subchain (including the effective interaction between slip-links), μ is the effective chemical potential which is determined to satisfy the condition $\langle n \rangle_{\text{eq}} = 1$. The single subchain free energy is given as follows:

$$\mathcal{F}_{\text{single}}(\mathbf{Q}, n) = \frac{\mathbf{Q}^2}{2n} + \left(\frac{3}{2} - \alpha \right) \ln n. \quad (55)$$

Here the parameter α represents the strength of the repulsive interaction between slip-links²⁰. The ideal and repulsive slip-link models correspond to $\alpha = 0$ and $3/2$, respectively. The equidistant slip-link model corresponds to the limit of $\alpha \rightarrow \infty$. The normalization constant for the probability given by eq (54) (the grand partition function) is calculated straightforwardly:

$$\int d\mathbf{Q} dn e^{-\mathcal{F}_{\text{single}}(\mathbf{Q}, n) - \mu n} = (2\pi)^{3/2} \mu^{-\alpha-1} \Gamma(\alpha + 1), \quad (56)$$

where $\Gamma(x)$ is the gamma function^{26,27}. From eqs (54) and (56), the equilibrium distribution function $P_{\text{eq,L}}(\mathbf{Q}, n)$ is rewritten as the following explicit form:

$$P_{\text{eq,L}}(\mathbf{Q}, n) = \frac{\mu^{\alpha+1}}{(2\pi)^{3/2} \Gamma(\alpha + 1)} n^{\alpha-3/2} e^{-\mathbf{Q}^2/2n - \mu n}. \quad (57)$$

The single-subchain level statistical properties can be calculated from eq (57). The segment number distribution function is obtained by integrating eq (57) over \mathbf{Q} :

$$P_{\text{eq,L}}(n) = \int d\mathbf{Q} P_{\text{eq,L}}(\mathbf{Q}, n) = \frac{\mu^{\alpha+1}}{\Gamma(\alpha + 1)} n^{\alpha} e^{-\mu n}. \quad (58)$$

Thus the equilibrium average of the segment number becomes

$$\langle n \rangle_{\text{eq}} = \int dn n P_{\text{eq,L}}(n) = \frac{\alpha + 1}{\mu}. \quad (59)$$

From the condition $\langle n \rangle_{\text{eq}} = 1$, we have the simple relation between μ and α , as $\mu = \alpha + 1$. Finally the segment number distribution (58) is rewritten as

$$P_{\text{eq,L}}(n) = \frac{(\alpha + 1)^{\alpha+1}}{\Gamma(\alpha + 1)} n^\alpha e^{-(\alpha+1)n}. \quad (60)$$

Eq (60) gives eq (17) in the main text. (At the limit of $\alpha \rightarrow \infty$, eq (60) approaches to the delta function.)

The bond vector distribution function is obtained by integrating eq (57) over n . For $\alpha = 0$, by using the variable transform $u = 1/\sqrt{n}$, we have

$$\begin{aligned} P_{\text{eq,IL}}(\mathbf{Q}) &= \frac{2}{(2\pi)^{3/2}} \int_0^\infty du e^{-\mathbf{Q}^2 u^2 / 2 - u^{-2}} \\ &= \frac{1}{4\pi|\mathbf{Q}|} \left[e^{\sqrt{2}|\mathbf{Q}|} \text{erf} \left(\frac{|\mathbf{Q}|u}{\sqrt{2}} + \frac{1}{u} \right) + e^{-\sqrt{2}|\mathbf{Q}|} \text{erf} \left(\frac{|\mathbf{Q}|u}{\sqrt{2}} - \frac{1}{u} \right) \right]_0^\infty \\ &= \frac{1}{2\pi|\mathbf{Q}|} e^{-\sqrt{2}|\mathbf{Q}|}, \end{aligned} \quad (61)$$

where $\text{erf}(x)$ is the error function and we have used the integral formula for the error function^{26,27}. For $\alpha = 3/2$, by introducing the variable transform $s = \ln(\sqrt{5}n/|\mathbf{Q}|)$, we have

$$\begin{aligned} P_{\text{eq,RL}}(\mathbf{Q}) &= \frac{25}{12\pi^2} |\mathbf{Q}| \int_{-\infty}^\infty ds e^{s - \sqrt{5}|\mathbf{Q}| \cosh s} \\ &= \frac{25}{6\pi^2} |\mathbf{Q}| K_1(\sqrt{5}|\mathbf{Q}|). \end{aligned} \quad (62)$$

Here we have utilized the integral representation of the modified Bessel function⁴⁶. For the equidistant slip-link model (at the limit of $\alpha \rightarrow \infty$), the n -dependent term in the integrand approaches to the delta function. Thus we simply have

$$P_{\text{eq,EL}}(\mathbf{Q}) = \frac{1}{(2\pi)^{3/2}} e^{-\mathbf{Q}^2/2}. \quad (63)$$

Eqs (61)-(63) give eq (19) in the main text.

B Characteristic Modulus

At $t = 0$, the shear relaxation modulus $G(t = 0)$ coincides to the characteristic modulus G_0 . This property is common for all the slip-link and slip-spring models examined in this work. Because $G(t = 0)$ is expressed as the equal-time correlation, it can be straightforwardly evaluated. For the slip-link models, we have

$$\begin{aligned} G_L(t = 0) &= \nu_0 \langle \hat{\sigma}_{xy}^2 \rangle_{\text{eq}} \\ &= \nu_0 \sum_{Z=1}^\infty \int d\{n_k\} \left[\int d\{\mathbf{R}_k\} \sum_{k=1}^Z \frac{Q_{k,x}^2 Q_{k,y}^2}{n_k^2} \prod_{k=1}^Z P_{\text{eq,L}}(\mathbf{R}_k | n_k) \right] P_{\text{eq,L}}(\{n_k\}, Z) \\ &= \nu_0 \sum_{Z=1}^\infty Z \int d\{n_k\} P_{\text{eq,L}}(\{n_k\}, Z) = G_0. \end{aligned} \quad (64)$$

On the other hand, for the slip-spring models, we have

$$\begin{aligned} G_S(t = 0) &= \nu_0 \langle \hat{\sigma}_{xy}^2 \rangle_{\text{eq}} + \nu_0 \langle \hat{\sigma}_{xy} \hat{\sigma}_{xy}^{(v)} \rangle_{\text{eq}} \\ &= G_0 + \nu_0 \sum_{Z=1}^\infty \int d\{n_k\} \left[\int d\{\mathbf{R}_k\} \sum_{k=1}^Z \frac{Q_{k,x} Q_{k,y}}{n_k} \prod_{k=1}^Z P_{\text{eq,S}}(\mathbf{R}_k | n_k) \right] \left[\int d\{\mathbf{R}_k\} \right. \\ &\quad \times \sum_{k=0}^Z \frac{(R_{k,x} - A_{k,x})(R_{k,y} - A_{k,y})}{\phi} P_{\text{eq,S}}(\{\mathbf{R}_k\}, \{\mathbf{A}_k\} | \{n_k\}, Z) \left. \right] P_{\text{eq,S}}(\{n_k\}, Z) \\ &= G_0. \end{aligned} \quad (65)$$

Therefore, for all models examined in this work, $G(t=0) = G_0$. Of course, in reality, $G(t=0)$ does not coincide to G_0 because there are fast relaxation modes such as the subchain-scale Rouse modes and segment (glassy) modes. The characteristic modulus calculated here ignores contributions of these fast modes, and only the entanglement modes are considered. The slip-link and slip-spring models examined in this work are coarse-grained models, and the fine scale relaxations (or fluctuations) are not explicitly taken into account. If we integrate some fast relaxation modes into the model, G_0 will be changed. (In this sense, one may interpret the characteristic modulus G_0 as a rather model dependent quantity.)

C Single-Subchain Statistics in Equidistant Slip-Spring Model

In this appendix, we show the detailed calculations for the single-subchain properties in the equidistant slip-spring model. In this model, the number of segments in a subchain is constant, and thus we do not need to consider the degrees of freedom for the segment numbers. (For sufficiently long chains, the effects of the chain ends become negligibly small. Thus we assume that the segment numbers in subchains at chain ends are also constant.) The equilibrium distribution function can be expressed as

$$P_{\text{eq,ES}}(\{\mathbf{R}_k\}, \{\mathbf{A}_k\}) \propto \exp \left[-\frac{1}{2} \sum_{k=1}^Z (\mathbf{R}_k - \mathbf{R}_{k-1})^2 - \frac{1}{2\phi} \sum_{k=0}^Z (\mathbf{R}_k - \mathbf{A}_k)^2 \right]. \quad (66)$$

In principle, we can obtain the probability distribution for a single subchain by integrating eq (66) over $\{\mathbf{R}_k\}$ except the target subchain. However, since all the anchoring points are (indirectly) connected (by the polymer chain), such an integration is not that simple. The difficulty mainly arises from the coupling between $\{\mathbf{R}_k\}$ and $\{\mathbf{A}_k\}$. The integral over $\{\mathbf{R}_k\}$ is a Gaussian integral over multiple variables, and we need to calculate the covariance matrix and its inverse. Unfortunately, the covariance matrix is not in a simple form in the current case.

Here we calculate the integral in an iterative manner, by starting from the chain end. The integral over \mathbf{R}_0 can be calculated straightforwardly:

$$\begin{aligned} & \int d\mathbf{R}_0 P_{\text{eq,ES}}(\{\mathbf{R}_k\}, \{\mathbf{A}_k\}) \\ & \propto \exp \left[-\frac{1}{2(1+\phi)} (\mathbf{R}_1 - \mathbf{A}_0)^2 - \frac{1}{2} \sum_{k=2}^Z (\mathbf{R}_k - \mathbf{R}_{k-1})^2 - \frac{1}{2\phi} \sum_{k=1}^Z (\mathbf{R}_k - \mathbf{A}_k)^2 \right] \\ & \propto \exp \left[-\frac{1}{2\bar{\phi}_1} (\mathbf{R}_1 - \bar{\mathbf{A}}_1)^2 - \frac{1}{2\phi} (\mathbf{A}_0^2 + \mathbf{A}_1^2) + \frac{1}{2\bar{\phi}_1} \bar{\mathbf{A}}_1^2 \right. \\ & \quad \left. - \frac{1}{2} \sum_{k=2}^Z (\mathbf{R}_k - \mathbf{R}_{k-1})^2 - \frac{1}{2\phi} \sum_{k=2}^Z (\mathbf{R}_k - \mathbf{A}_k)^2 \right], \end{aligned} \quad (67)$$

with

$$\frac{1}{\bar{\phi}_1} \equiv \frac{1}{\phi} + \frac{1}{1+\phi}, \quad (68)$$

$$\bar{\mathbf{A}}_1 \equiv \frac{\bar{\phi}_1}{\phi} \mathbf{A}_1 + \left(\frac{\bar{\phi}_1}{\phi} - 1 \right) \mathbf{A}_0. \quad (69)$$

We may interpret eq (67) as the change of the anchoring point and the slip-spring size for \mathbf{R}_1 . Eqs (68) and (69) give the effective anchoring position and the slip-spring size. Then we can integrate eq (67) over \mathbf{R}_2 in the same manner. In eq (67), only the terms which contain \mathbf{R}_0 and \mathbf{R}_1 are changed and other terms are unchanged. The terms which do not depend on \mathbf{R}_2 never affect the integral over \mathbf{R}_2 . Therefore, we can safely ignore most of terms when we calculate the

integral. If we have performed the multiple integrals over $\mathbf{R}_0, \mathbf{R}_1, \dots, \mathbf{R}_{j-1}$, we should have

$$\begin{aligned} & \int d\mathbf{R}_0 d\mathbf{R}_1 \dots d\mathbf{R}_{j-1} P_{\text{eq,ES}}(\{\mathbf{R}_k\}, \{\mathbf{A}_k\}) \\ & \propto \exp \left[-\frac{1}{2\bar{\phi}_j} (\mathbf{R}_j - \bar{\mathbf{A}}_j)^2 - \frac{1}{2} (\mathbf{R}_j - \mathbf{R}_{j+1})^2 - \frac{1}{2\phi} (\mathbf{R}_{j+1} - \bar{\mathbf{A}}_{j+1})^2 - \dots \right], \end{aligned} \quad (70)$$

and the multiple integrals over $\mathbf{R}_0, \mathbf{R}_1, \dots, \mathbf{R}_j$ become

$$\begin{aligned} & \int d\mathbf{R}_0 d\mathbf{R}_1 \dots d\mathbf{R}_j P_{\text{eq,ES}}(\{\mathbf{R}_k\}, \{\mathbf{A}_k\}) \\ & \propto \int d\mathbf{R}_j \exp \left[-\frac{1}{2(1+\bar{\phi}_j)} (\mathbf{R}_{j+1} - \bar{\mathbf{A}}_j)^2 - \frac{1}{2\phi} (\mathbf{R}_{j+1} - \bar{\mathbf{A}}_{j+1})^2 - \dots \right] \\ & \propto \exp \left[-\frac{1}{2} \left(\frac{1}{\phi} + \frac{1}{1+\bar{\phi}_j} \right) \left[\mathbf{R}_{j+1} - \frac{\mathbf{A}_{j+1}/\phi + \bar{\mathbf{A}}_j/(1+\bar{\phi}_j)}{1/\phi + 1/(1+\bar{\phi}_j)} \right]^2 - \dots \right]. \end{aligned} \quad (71)$$

From eq (71), we find the following recurrence relations for the effective anchoring point and the slip-spring size:

$$\frac{1}{\bar{\phi}_{j+1}} = \frac{1}{\phi} + \frac{1}{1+\bar{\phi}_j}, \quad (72)$$

$$\bar{\mathbf{A}}_{j+1} = \frac{\mathbf{A}_{j+1}/\phi + \bar{\mathbf{A}}_j/(1+\bar{\phi}_j)}{1/\phi + 1/(1+\bar{\phi}_j)} = \frac{\bar{\phi}_{j+1}}{\phi} \mathbf{A}_{j+1} + \left(1 - \frac{\bar{\phi}_{j+1}}{\phi} \right) \bar{\mathbf{A}}_j. \quad (73)$$

The “initial” conditions are $\phi_0 = \phi$ and $\bar{\mathbf{A}}_0 = \mathbf{A}_0$. The integral can be performed in the opposite direction, from another chain end ($j = Z$). In this case, we have the effective slip-spring size $\bar{\phi}_j^\dagger$ and the effective anchoring point $\bar{\mathbf{A}}_j^\dagger$ which satisfy

$$\frac{1}{\bar{\phi}_{j-1}^\dagger} = \frac{1}{\phi} + \frac{1}{1+\bar{\phi}_j^\dagger}, \quad (74)$$

$$\bar{\mathbf{A}}_{j-1}^\dagger = \frac{\bar{\phi}_{j-1}^\dagger}{\phi} \mathbf{A}_{j-1} + \left(1 - \frac{\bar{\phi}_{j-1}^\dagger}{\phi} \right) \bar{\mathbf{A}}_j^\dagger, \quad (75)$$

with the “initial” conditions $\bar{\phi}_Z^\dagger = \phi$ and $\bar{\mathbf{A}}_Z^\dagger = \mathbf{A}_Z$.

The recurrence relations (72)-(75) are not easy to solve analytically. Thus we seek approximate solutions, instead of the exact solutions. For a sufficiently long chain, the effective slip-spring size approximately becomes constant, $\bar{\phi}_j \approx \bar{\phi}_\infty$, where $\bar{\phi}_\infty$ is defined via

$$\frac{1}{\bar{\phi}_\infty} = \frac{1}{\phi} + \frac{1}{1+\bar{\phi}_\infty}. \quad (76)$$

The solution of eq (76) is

$$\bar{\phi}_\infty = \frac{-1 + \sqrt{1+4\phi}}{2}. \quad (77)$$

The recurrence relation (73) can be also approximated as

$$\bar{\mathbf{A}}_{j+1} \approx \frac{\bar{\phi}_\infty}{\phi} \mathbf{A}_{j+1} + \left(1 - \frac{\bar{\phi}_\infty}{\phi} \right) \bar{\mathbf{A}}_j, \quad (78)$$

and eq (78) can be easily solved:

$$\bar{\mathbf{A}}_j \approx \frac{\bar{\phi}_\infty}{\phi} \sum_{k=0}^{\infty} \left(1 - \frac{\bar{\phi}_\infty}{\phi} \right)^k \mathbf{A}_{j-k}. \quad (79)$$

In a similar way, we have the approximate solutions for $\bar{\phi}_j^\dagger$ and $\bar{\mathbf{A}}_j^\dagger$: $\bar{\phi}_j^\dagger \approx \bar{\phi}_\infty$ and

$$\bar{\mathbf{A}}_j^\dagger \approx \frac{\bar{\phi}_\infty}{\phi} \sum_{k=0}^{\infty} \left(1 - \frac{\bar{\phi}_\infty}{\phi}\right)^j \mathbf{A}_{j+k}. \quad (80)$$

Under these approximations, finally, the probability distribution for a single subchain is given as

$$P_{\text{eq,ES}}(\mathbf{R}_{k-1}, \mathbf{R}_k, \{\mathbf{A}_k\}) \propto \exp \left[-\frac{(\mathbf{R}_k - \mathbf{R}_{k-1})^2}{2} - \frac{(\mathbf{R}_{k-1} - \bar{\mathbf{A}}_{k-1})^2}{2\bar{\phi}_\infty} - \frac{(\mathbf{R}_k - \bar{\mathbf{A}}_k^\dagger)^2}{2\bar{\phi}_\infty} + \dots \right], \quad (81)$$

and the conditional probability distribution for \mathbf{R}_{k-1} and \mathbf{R}_k becomes

$$P_{\text{eq,ES}}(\mathbf{R}_{k-1}, \mathbf{R}_k | \{\mathbf{A}_k\}) = \frac{(1 + 2\bar{\phi}_\infty)^{3/2}}{(2\pi\bar{\phi}_\infty)^3} \exp \left[-\frac{(\mathbf{R}_k - \mathbf{R}_{k-1})^2}{2} - \frac{(\mathbf{R}_{k-1} - \bar{\mathbf{A}}_{k-1})^2}{2\bar{\phi}_\infty} - \frac{(\mathbf{R}_k - \bar{\mathbf{A}}_k^\dagger)^2}{2\bar{\phi}_\infty} + \frac{(\bar{\mathbf{A}}_k - \bar{\mathbf{A}}_k^\dagger)^2}{1 + 2\bar{\phi}_\infty} \right]. \quad (82)$$

Thus we have eqs (25)-(28) in the main text.

To calculate the statistical averages, we need the probability distribution for the anchoring points $\{\mathbf{A}_k\}$. Unfortunately, the anchoring point distribution function itself becomes rather complicated and difficult to handle. However, since eq (66) is a Gaussian distribution, some statistical averages can be directly calculated without explicitly calculating the probability distribution function. We consider some statistical properties of the vectors which connect two neighboring anchoring points, $\mathbf{U}_k \equiv \mathbf{A}_k - \mathbf{A}_{k-1}$. This would be interpreted as the bond vector for the anchoring points. The probability distribution for two neighboring anchoring points can be calculated straightforwardly:

$$P_{\text{eq,ES}}(\mathbf{A}_{k-1}, \mathbf{A}_k) \propto \int d\mathbf{R}_{k-1} d\mathbf{R}_k \exp \left[-\frac{(\mathbf{R}_k - \mathbf{R}_{k-1})^2}{2} - \frac{(\mathbf{R}_{k-1} - \mathbf{A}_{k-1})^2}{2\phi} - \frac{(\mathbf{R}_k - \mathbf{A}_k)^2}{2\phi} \right] \\ \propto \exp \left[-\frac{\mathbf{U}_k^2}{2(1+2\phi)} \right]. \quad (83)$$

Thus we have $\langle \mathbf{U}_k \rangle_{\text{eq}} = 0$, and $\langle \mathbf{U}_k \mathbf{U}_k \rangle_{\text{eq}} = (1 + 2\phi)\mathbf{1}$. Two bond vectors \mathbf{U}_k and \mathbf{U}_j are not statistically correlated if they do not share at least one anchoring point. Thus we have $\langle \mathbf{U}_k \mathbf{U}_j \rangle_{\text{eq}} = 0$ if $|j - k| > 1$. If two bond vectors share one anchoring point ($j = k \pm 1$) we need the probability distribution for three sequential anchoring points to calculate the correlation:

$$P_{\text{eq,ES}}(\mathbf{A}_{k-1}, \mathbf{A}_k, \mathbf{A}_{k+1}) \propto \int d\mathbf{R}_{k-1} d\mathbf{R}_k d\mathbf{R}_{k+1} \exp \left[-\frac{(\mathbf{R}_k - \mathbf{R}_{k-1})^2}{2} - \frac{(\mathbf{R}_{k+1} - \mathbf{R}_k)^2}{2} - \frac{(\mathbf{R}_{k-1} - \mathbf{A}_{k-1})^2}{2\phi} - \frac{(\mathbf{R}_k - \mathbf{A}_k)^2}{2\phi} - \frac{(\mathbf{R}_{k+1} - \mathbf{A}_{k+1})^2}{2\phi} \right] \\ \propto \exp \left[-\frac{1}{2} [\mathbf{U}_k \quad \mathbf{U}_{k+1}] \cdot \mathbf{C}^{-1} \cdot \begin{bmatrix} \mathbf{U}_k \\ \mathbf{U}_{k+1} \end{bmatrix} \right], \quad (84)$$

where \mathbf{C}^{-1} is the inverse of the covariance matrix,

$$\mathbf{C}^{-1} = \frac{1}{(1+\phi)(1+3\phi)} \begin{bmatrix} (1+2\phi)\mathbf{1} & \phi\mathbf{1} \\ \phi\mathbf{1} & (1+2\phi)\mathbf{1} \end{bmatrix}. \quad (85)$$

By inverting eq (85), the covariance matrix \mathbf{C} becomes

$$\mathbf{C} = \begin{bmatrix} (1+2\phi)\mathbf{1} & -\phi\mathbf{1} \\ -\phi\mathbf{1} & (1+2\phi)\mathbf{1} \end{bmatrix}, \quad (86)$$

and thus we have $\langle \mathbf{U}_k \mathbf{U}_{k\pm 1} \rangle_{\text{eq}} = -\phi\mathbf{1}$. By combining these results, we have eq (42) in the main text.

References

- [1] Doi, M.; Edwards, S. F. *The Theory of Polymer Dynamics*; Oxford University Press: Oxford, 1986.
- [2] Fetters, L. J.; Lohse, D. J.; Colby, R. H. In *Chain Dimensions and Entanglement Spacings*; Mark, J. E., Ed.; Chapter 25, pp 445–452, in *Physical Properties of Polymers Handbook*, J. E. Mark ed, 2nd ed. (Springer, New York, 2007).
- [3] Liu, C.; He, J.; van Ruymbeke, E.; Keunings, R.; Bailly, C. Evaluation of different methods for the determination of the plateau modulus and the entanglement molecular weight. *Polymer* **2006**, *47*, 4461–4479.
- [4] Steenbakkers, R. J. A.; Tzoumanekas, C.; Li, Y.; Liu, W. K.; Kröger, M.; Schieber, J. D. Primitive-path statistics of entangled polymers: mapping multi-chain simulations onto single-chain mean-field models. *New J. Phys.* **2014**, *16*, 051027.
- [5] Masubuchi, Y.; Ianniruberto, G.; Greco, F.; Marrucci, G. Quantitative comparison of primitive chain network simulations with literature data of linear viscoelasticity for polymer melts. *J. Non-Newtonian Fluid Mech.* **2008**, *149*, 87–92.
- [6] Masubuchi, Y.; Uneyama, T. Comparison among multi-chain models for entangled polymer dynamics. *Soft Matter* **2018**, *14*, 5986–5994.
- [7] Everaers, R. Entanglement effects in defect-free model polymer networks. *New J. Phys.* **1999**, *1*, 12.
- [8] Masubuchi, Y.; Ianniruberto, G.; Greco, F.; Marrucci, G. Entanglement molecular weight and frequency response of sliplink networks. *J. Chem. Phys.* **2003**, *119*, 6925–6930.
- [9] Likhtman, A. E.; McLeish, T. C. B. Quantitative Theory for Linear Dynamics of Linear Entangled Polymers. *Macromolecules* **2002**, *35*, 6332–6343.
- [10] Larson, R. G.; Sridhar, T.; Leal, L. G.; McKinley, G. H.; Likhtman, A. E.; McLeish, T. C. B. Definitions of entanglement spacing and time constants in the tube model. *J. Rheol.* **2003**, *47*, 809–818.
- [11] Hua, C. C.; Schieber, J. D. Segment connectivity, chain-length breathing, segmental stretch, and constraint release in reptation models. I. Theory and single-step strain predictions. *J. Chem. Phys.* **1998**, *109*, 10018–10027.
- [12] Masubuchi, Y.; Takimoto, J.; Koyama, K.; Ianniruberto, G.; Greco, F.; Marrucci, G. Brownian simulations of a network of reptating primitive chains. *J. Chem. Phys.* **2001**, *115*, 4387–4394.
- [13] Doi, M.; Takimoto, J. Molecular modelling of entanglement. *Phil. Trans. R. Soc. Lond. A* **2003**, *361*, 641–650.
- [14] Likhtman, A. E. Single-Chain Slip-Link Model of Entangled Polymers: Simultaneous Description of Neutron Spin-Echo, Rheology, and Diffusion. *Macromolecules* **2005**, *38*, 6128–6139.
- [15] Nair, D. M.; Schieber, J. D. Linear Viscoelastic Predictions of a Consistently Unconstrained Brownian Slip-Link Model. *Macromolecules* **2006**, *39*, 3386–3397.
- [16] Chappa, V. C.; Morse, D. C.; Zippelius, A.; Müller, M. Translationally Invariant Slip-Spring Model for Entangled Polymer Dynamics. *Phys. Rev. Lett.* **2012**, *109*, 148302.
- [17] Uneyama, T.; Masubuchi, Y. Multi-chain slip-spring model for entangled polymer dynamics. *J. Chem. Phys.* **2012**, *137*, 154902.
- [18] Shanbhag, S. Fast Slip Link Model for Bidisperse Linear Polymer Melts. *Macromolecules* **2019**, *52*, 3092–3103.

- [19] Shanbhag, S. Mathematical foundations of an ultra coarse-grained slip link model. *J. Chem. Phys.* **2019**, *151*, 044903.
- [20] Uneyama, T.; Masubuchi, Y. Detailed Balance Condition and Effective Free Energy in the Primitive Chain Network Model. *J. Chem. Phys.* **2011**, *135*, 184904.
- [21] Schieber, J. D. Fluctuations in entanglements of polymer liquids. *J. Chem. Phys.* **2003**, *118*, 5162–5166.
- [22] Bateman, H. *Higher Transcendental Functions*; McGraw-Hill: New York, 1955; Vol. 3.
- [23] Evans, D. J.; Morris, G. P. *Statistical Mechanics of Nonequilibrium Liquids*, 2nd ed.; Cambridge University Press: Cambridge, 2008.
- [24] Ramirez, J.; Sukumaran, S. K.; Likhtman, A. E. Significance of cross correlations in the stress relaxation of polymer melts. *J. Chem. Phys.* **2007**, *126*, 244904.
- [25] Uneyama, T. Single Chain Slip-Spring Model for Fast Rheology Simulations of Entangled Polymers on GPU. *Nihon Reoroji Gakkaishi (J. Soc. Rheol. Jpn.)* **2011**, *39*, 135–152.
- [26] Abramowitz, M., Stegun, I. A., Eds. *Handbook of Mathematical Functions with Formulas, Graphs, and Mathematical Tables*, 10th ed.; Dover: New York, 1972.
- [27] Olver, F. W. J., Lozier, D. W., Boisvert, R. F., Clark, C. W., Eds. *NIST Handbook of Mathematical Functions*; Cambridge University Press, 2010.
- [28] Rubinstein, M.; Panyukov, S. Nonaffine Deformation and Elasticity of Polymer Networks. *Macromolecules* **1997**, *30*, 8036–8044.
- [29] Rubinstein, M.; Panyukov, S. Elasticity of Polymer Networks. *Macromolecules* **2002**, *35*, 6670–6686.
- [30] Matsumoto, M.; Nishimura, T. Mersenne twister: a 623-dimensionally equidistributed uniform pseudo-random number generator. *ACM Trans. Model. Comp. Simul.* **1998**, *8*, 3–30, <http://www.math.sci.hiroshima-u.ac.jp/~m-mat/MT/emt.html>.
- [31] Devroye, L. *Non-Uniform Random Variate Generation*; Springer: New York, 1986.
- [32] Marsaglia, G.; Tsang, W. W. A Simple Method for Generating Gamma Variables. *ACM Trans. Math. Software* **2000**, *26*, 363–372.
- [33] Everaers, R. Topological versus rheological entanglement length in primitive-path analysis protocols, tube models, and slip-link models. *Phys. Rev. E* **2012**, *86*, 022801.
- [34] Masubuchi, Y.; Doi, Y.; Uneyama, T. Multi-chain slip-spring simulations with various slip-spring densities. arXiv:2011.03222.
- [35] Masubuchi, Y. Multichain Slip-Spring Simulations for Branch Polymers. *Macromolecules* **2018**, *51*, 10184–10193.
- [36] Masubuchi, Y.; Uneyama, T. Multi-chain slip-spring simulations for polyisoprene melts. *Korea-Australia Rheology Journal* **2019**, *31*, 241–248.
- [37] Everaers, R.; Sukumaran, S. K.; Grest, G. S.; Svaneborg, C.; Sivasubramanian, A.; Kremer, K. Rheology and Microscopic Topology of Entangled Polymeric Liquids. *Science* **2004**, *303*, 823.
- [38] Sukumaran, S. K.; Grest, G. S.; Kremer, K.; Everaers, R. Identifying the Primitive Path Mesh in Entangled Polymer Liquids. *J. Polym. Sci. B: Polym. Phys.* **2005**, *43*, 917–933.
- [39] Kröger, M. Shortest multiple disconnected path for the analysis of entanglements in two- and three-dimensional polymeric systems. *Comp. Phys. Comm.* **2005**, *168*, 209–232.

- [40] Tzoumanekas, C.; Theodorou, D. N. Topological Analysis of Linear Polymer Melts: A Statistical Approach. *Macromolecules* **2006**, *39*, 4592–4604.
- [41] Becerra, D.; Córdoba, A.; Katzarova, M.; Andreev, M.; Venerus, D. C.; Schieber, J. D. Polymer rheology predictions from first principles using the slip-link model. *J. Rheol.* **2020**, *64*, 1035.
- [42] Doi, M. Explanation for the 3.4-power law for viscosity of polymeric liquids on the basis of the tube model. *J. Polym. Sci.: Polym. Phys. Ed.* **1983**, *21*, 667–684.
- [43] Fetters, L. J.; Lohse, D. J.; Graessley, W. W. Chain Dimensions and Entanglement Spacings in Dense Macromolecular Systems. *J. Polym. Sci. B: Polym. Phys.* **1999**, *37*, 1023–1033.
- [44] Osaki, K. A Note on Rheology of Polymeric Systems. *Nihon Reoroji Gakkaishi (J. Soc. Rheol. Jpn.)* **2002**, *30*, 165–172, in Japanese.
- [45] Greco, F. Equilibrium statistical distributions for subchains in an entangled polymer melt. *Eur. Phys. J. E* **2008**, *25*, 175–180.
- [46] Lebedev, N. N. *Special Functions and Their Applications*; Dover: New York, 1972.